S-429

Draft version

S-429

Progress Report on Neutron Physics Research in Sweden

AKTIEBOLAGET ATOMENERGI

STUDSVIK, NYKÖPING, SWEDEN 1971

Draft version

PROGRESS REPORT ON NEUTRON PHYSICS RESEARCH IN SWEDEN

Compiled by
H. Condé
Research Institute of National Defence
Stockholm, Sweden
and
T. Wiedling
Neutron Physics Section
Atomic Energy Company
Studsvik
Nyköping, Sweden

April 1971

CONTENTS

PREFACE

Information on neutron physics activities in progress in different laboratories in Sweden are collected in this progress report. However, the present INDC report is to be followed shortly by an EANDC report which will largely contain the same information. From a practical point of view it is considered quite inconvenient to present two completely separate documents. Thus the present report can be regarded as the first (draft) edition to be followed by a second, more or less revised, version which is the EANDC report.

LABORATORIES SUBMITTING CONTRIBUTIONS TO THIS COMPILATION

I. NEUTRON PHYSICS

I.1. ELASTIC AND INELASTIC NEUTRON SCATTERING

I.1.1. Optical model analyses of neutron scattering at 8 MeV

B. Holmqvist and T. Wiedling
Atomic Energy Company, Studsvik, Nyköping

The purpose of the present investigation was to measure differential neutron elastic scattering cross sections at 8 MeV for several elements in the mass interval A=27-209. This is a continuation of work which has been done at our laboratory for several years. Throughout, the work has been oriented toward the need for cross section data for application to reactor physics problems. However, the interpretation of the observations in terms of an optical model potential with five adjustable parameters shows that the experimental data can be well described by this model. A good basis is thus obtained for a general description of neutron-nuclear interactions covering a large mass range. By extracting information from neutron scattering data some evidence has previously been obtained that the spherical optical potential should be dependent on the isobaric spin [1, 2]. The present study will contribute further knowledge supporting the existence of an isobaric spin term in the optical potential.

The experimental details have been described elsewhere [2]. However, for completeness the experimental parameters are summarized in Table I.

The observed angular distributions have been compared with distributions calculated with a local nuclear optical potential of the form

$$-V(r) = Uf(r) + iWg(r) + U_{so}\left(\frac{\hbar}{\mu_\pi c}\right)^2 \frac{1}{r}\frac{d}{dr}\,|f(r)|\,\bar{\sigma}\cdot\bar{\ell}.$$

The radial variation of the real potential is determined by the Saxon-Woods form factor f(r) and that of the imaginary potential by the derivative Saxon-Woods form factor g(r). The corresponding

---

[1] Holmqvist, B. and Wiedling, T., Evidence for a symmetry term in the optical potential for neutrons. Phys. Letters 26 B (1968) 620.

[2] Holmqvist, B., A systematic study of fast neutron elastic scattering in the energy region 1.5 to 8.1 MeV. Arkiv Fysik 38 (1968) 403.

strengths of these potentials are U and W, respecively. The last term of the potential takes the spin-orbit interaction into account. Its strength is U_{so}. The real and imaginary radii are defined by the expressions $R_U = r_{oU}A^{1/3}$ and $R_W = r_{oW}A^{1/3}$. The diffuseness of the real and imaginary potential terms are determined by the parameters a and b, respectively.

Five of the potential parameters, i.e. U, W, r_{oU}, r_{oW} and a have been adjusted to obtain the best agreement with the measured elastic cross sections. The best fits to the experimental data have been acquired by using the ABACUS II automatic five-parameter search code. The spin-orbit potential depth was kept constant as also was the diffuseness parameter of the imaginary potential since the angular distributions are comparatively insensitive to variations in these parameters [2]. Their values were chosen to be 8.0 MeV and 0.48 fm, respectively.

The compound elastic cross sections are negligible for all the elements at 8 MeV neutron energy.

The measured angular distributions as well as those calculated with the five-parameter search procedure are shown in Fig. 1. It is clear that the experimental distributions are well described by distributions calculated with the simple spherical optical potential. Even the calculated distributions of the light elements Al, S and Ca agree surprisingly well with the measured ones.

The optimum potential parameters corresponding to the best agreements between the experimental and calculated angular distributions have been plotted versus the mass number in Fig. 2. The geometrical parameters of the potential show no pronounced variations with the mass number except may be for r_{oW} which shows a tendency to increase somewhat with A. The real potential depth slowly decreases with A which is the case also for the imaginary potential at least for $A > 55$. Below that value the imaginary potential depth exhibits pronounced fluctuations.

Since the geometrical parameters have been obtained for a rather large number of elements and are essentially independent of A they have been used for mean value calculations representative of neutron scattering at 8 MeV in the mass interval $27 \leq A \leq 209$. The values obtained are: $\bar{r}_{oU} = 1.22 \pm 0.01$ fm, $\bar{r}_{oW} = 1.23 \pm 0.01$ fm

and $\bar{a} = 0.67 \pm 0.01$ fm. These values are in good agreement with those ($\bar{r}_{oU} = \bar{r}_{oW} = 1.21 \pm 0.01$ fm and $\bar{a} = 0.66 \pm 0.01$ fm) obtained previously from a study of neutron scattering in the energy interval 1.5 to 8.1 MeV [2].

Using the mean values of the geometrical parameters, analyses in terms of two variable parameters, namely the well depths U and W, have been performed. The best fits are not essentially different from those of the five parameter analyses and the differences are hardly visible on the scale of Fig. 1.

The optimum values of U and W from the two parameter calculations have been plotted in Fig. 2. It is seen that U and W obtained from the two analyses vary in the same way with A. However, the values of U obtained from the two parameter analyses show a smoother variation with A than those obtained from the five parameter analyses.

The values of the parameters U and W have been plotted versus the symmetry parameter $\alpha = (N - Z)/A$ in Fig. 3 showing that U decreases smoothly with α in contrast to W which exhibits a large scatter. It is clear that the real part of the optical potential contains an isobaric spin dependent potential part. Its strength is conveniently determined from the expression $U = U_0 - U_1 (N - Z)/A$ where U_0 and U_1 are constants [1]. A least squares fitting gives a value of 50 ± 10 MeV for U_1. However, because of the well-known ambiguity of U due to its dependence on r_{oU} it must be considered more correct to use the volume integral (J) of the real potential as a measure of its strength than U itself in a study of the α dependence [2]. Thus the quantity $JU/A = 4\pi U/A \int_0^\infty f(r)\, r^2 dr$ was calculated from the data of the five parameter analyses. The values of JU/A have been plotted versus α in Fig. 4. A comparison between Figs. 3 and 4 shows that the fluctuations of JU/A are smaller than those of U. Assuming that JU/A is linearly dependent on α the strength of the isobaric spin potential has been calculated to be 470 ± 40 MeV(fm)^3. No isobaric spin dependence of W has been extracted from the data because of the large fluctuations of W with (N - Z)/A.

TABLE I. The experimental parameters characteristic of the elastic scattering cross section measurements

Neutron source	$D(d,n)He^3$
Neutron energy	8.05 MeV
Gas target	Length of gas target cell 3 cm Nickel foil thickness 2.5 mg/cm^2 Deuterium gas pressure in the cell 1 kp/cm^2 Total energy spread $\pm$ 90 keV
Accelerator beam	Beam pulse frequency 1 MHz Beam pulse width at half-height 2 ns Mean target current 1.5 μA
Sample size and purity	Al to Bi, cylinders having lengths of 5.0 cm, 0.95 cm inner diameter and 2.5 cm outer diameter Polythene scatterer, 3.0 cm in length, 0.95 cm outer diameter and 0.65 cm inner diameter Sample purity $\geq$ 99.5%
Target-scatterer-detector distances	Target-scatterer 10 cm Scatterer-detector 300 cm
Neutron time-of-flight detector	Scintillators NE102A and NE104 Scintillator size 10 cm diameter and 5 cm length Spectrometer time resolution 3 ns
Neutron flux measurements	The neutron flux was monitored with a directional long counter
Angular interval	The angular distributions have been measured in the angular region 20° to 160° in 10° steps except in the forward directions, where measurements were performed in 5° steps
Background conditions	The signal-to-background ratio at the position of the elastic peak was 7 to 1 in the most unfavourable case i.e. at the forward scattering angles
Counting statistics	Statistical errors for the number of counts in the elastic peaks of the time-of-flight spectra $\leq$ 2% Statistical error for the number of monitor counts 0.3%
Errors	The experimental cross section errors are about 5 per cent

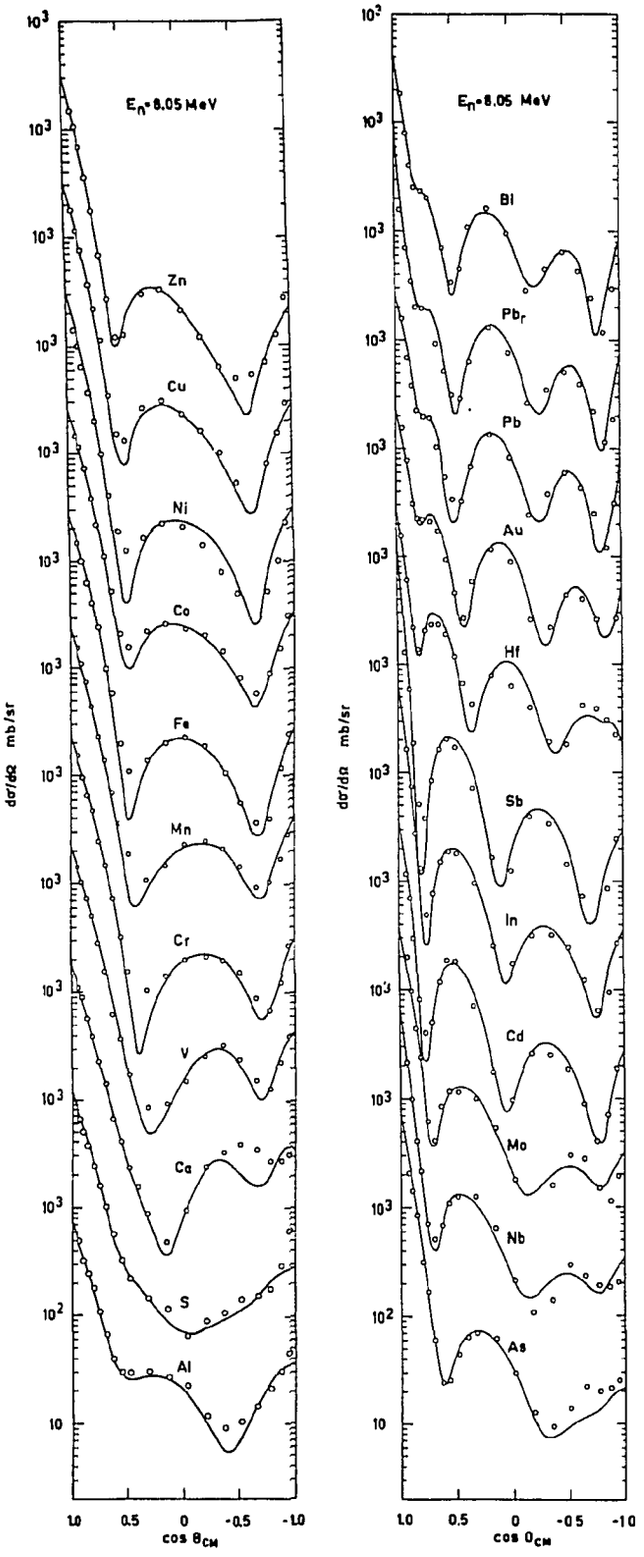

Fig. 1 The experimental (circles) and calculated (solid lines) angular distributions of elastically scattered 8.05 MeV neutrons.

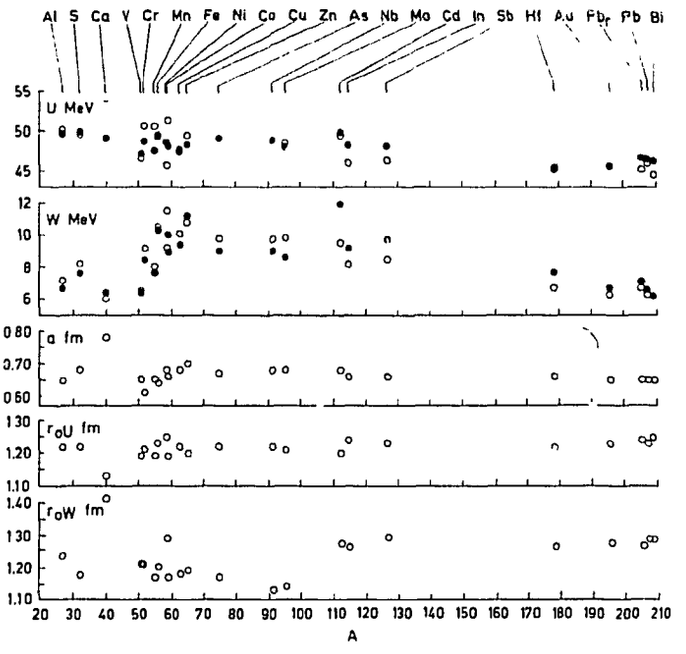

Fig. 2 The parameter values U, W, a, r_{oU} and r_{oW} plotted versus the mass number A. The values of U and W obtained by two and five parameter analyses are demonstrated (filled and open circles, respectively).

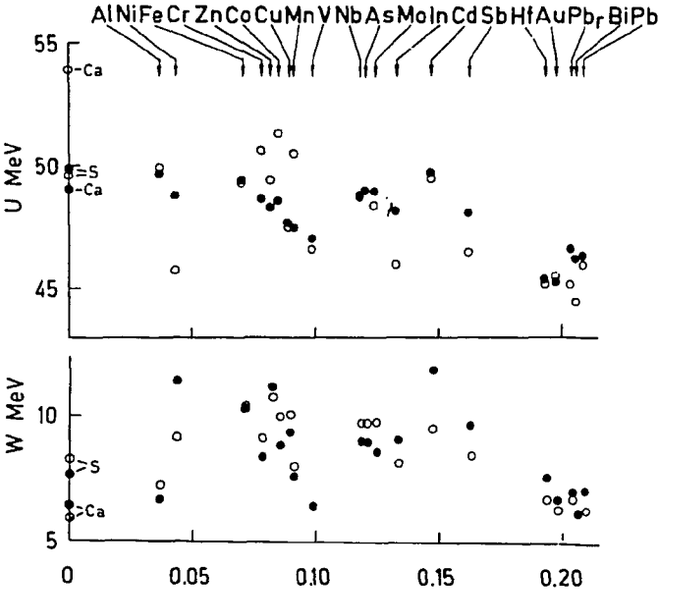

Fig. 3 The optimum values of U and W from the two parameter (filled circles) and five parameter (circles) analyses plotted as functions of the symmetry parameter (N - Z)/A.

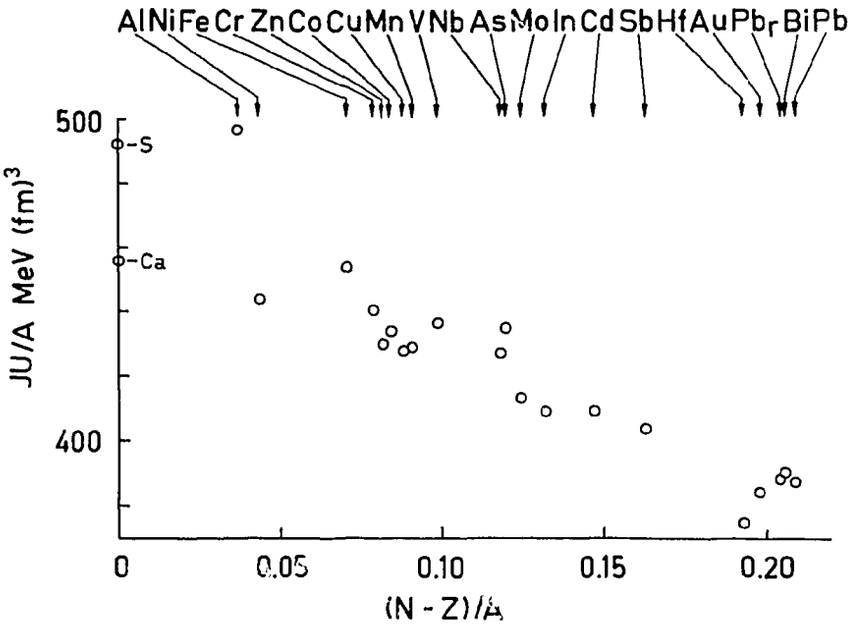

Fig. 4 The quantity JU/A plotted as a function of the symmetry parameter (N - Z)/A.

I.1.2. Neutron elastic scattering cross sections of vanadium, chromium, iron and nickel

B. Holmqvist and T. Wiedling
Atomic Energy Company, Studsvik, Nyköping

This work forms part of a neutron elastic scattering programme in the mass number region from the lightest to the very heaviest natural elements which has been going on for several years at our laboratory. The objective is the acquisition of cross section data at incident neutron energies between 1.8 and 8.1 MeV for reactor physics applications and the continuation of systematic investigations [1 - 3] of the characteristics of the optical model potential. Emphasis has been given to the important reactor constructional materials V, Cr, Fe and Ni for which elastic scattering angular distributions were measured at several energies in the above mentioned energy interval. Elastic scattering cross sections are requested [4] for these elements in the energy region 1 - 15 MeV in energy steps of about 50 keV in the low energy region and in steps of up to several hundred keV at higher energies. The angular distribution recordings are required at intervals of 5^{o} to 10^{o}.

The angular distribution measurements were carried out concurrently with those reported earlier [1 - 3]. The cross sections were measured relative to the n-p cross sections [5].

---

[1] Holmqvist, B., A systematic study of fast neutron elastic scattering in the energy region 1.5 to 8.1 MeV. Arkiv Fysik 38 (1968) 403.

[2] Holmqvist, B. and Wiedling, T., Neutron elastic scattering cross sections experimental data and optical model cross section calculations. 1969. (AE-366).

[3] Holmqvist, B., et.al., Fast neutron elastic and inelastic scattering of vanadium. 1969. (AE-375).

[4] Häussermann, W. and Schwarz, S., RENDA. Compilation of EANDC requests for neutron data measurements. 1968. (EANDC 61 "U").

[5] Horsley, A., Neutron cross sections of hydrogen in the energy range 0.0001 eV - 20 MeV. Nucl. Data A2 (1966) 243.

The experimental parameters and data characteristic of the elastic cross section measurements are collected in Table I.

Corrections of the experimental angular distributions have been applied for neutron multiple scattering in the sample under investigation as well as for neutron attenuation and geometrical effects caused by the size of the sample and its distances from target and detector [6].

The corrected experimental angular distributions are shown in Fig. 1. The cross sections for V are from reference [3], those of Cr at 2.47 MeV and higher energies are from references [1, 2] as are those at 3.0 MeV and higher energies for Fe and Ni.

The experimental elastic scattering angular distributions have been compared with cross sections calculated by using a local nuclear optical potential of the form

$$-V(r) = Uf(r) + iWg(r) + U_{so}\left(\frac{\hbar}{\mu_\pi c}\right)^2 \frac{1}{r}\frac{d}{dr}\left|f(r)\right| \bar{\sigma}\cdot\bar{\ell}$$

where U and W are the real and imaginary potential depths respectively and U_{so} the strength of the spin-orbit interaction. The diffuseness functions f(r) and g(r) are of the Saxon-Woods and derivative Saxon-Woods forms. The real and imaginary radii are defined by the relations $R_U = r_{oU} A^{1/3}$ and $R_W = r_{oW} A^{1/3}$, respectively. The corresponding diffuseness parameters are a and b.

The effect of compound elastic scattering has been calculated by applying the Hauser and Feshbach formalism together with the techniques described in reference [1]. The cross sections calculated with the Hauser and Feshbach theory have been corrected for level-width fluctuations according to Moldauer.

The calculations with the optical potential have been performed in two different manners depending upon the incident neutron energy. Thus the optical potential parameters, i.e. U, W, r_{oU}, r_{oW} and a corresponding to the best fits to the experimental data, have been obtained by using the ABACUS II automatic five-parameter search

---

[6] Holmqvist, B., Gustavsson, B. and Wiedling, T., A Monte Carlo program for calculation of neutron attenuation and multiple scattering corrections. Arkiv Fysik 34 (1967) 481.

routine except below 3 MeV neutron energy for the elements Fe and Ni and below 2.5 MeV for Cr where no parameter search procedures have been applied since resonance effects may be expected. But since it is of interest to obtain information concerning the ability of the optical model to describe the experimental results, potential depths were obtained in the low energy range 1.77 to 2.76 MeV by extrapolating the U and W values calculated for Cr, Fe and Ni at higher energies by the parameter search procedure. A least squares fit analysis was made for that purpose. The U-values were calculated from the relations, Cr: $U = 54.0 - 0.65\ E_n$, Fe: $U = 54.3 - 0.80\ E_n$ and Ni: $U = 58.7 - 1.60\ E_n$. The geometrical parameters, i.e. r_{oU}, r_{oW} and a, were taken to represent mean values for all energies studied in the five-parameter analyses. The values of b and U_{so} used throughout the calculations were 0.48 fm and 8 MeV, respectively. The parameters obtained from the search procedure of V, Cr, Fe and Ni are given in Tables II to V and the extrapolated optical potential parameters of Cr, Fe and Ni in Tables VI to VIII.

The calculated differential elastic scattering angular distributions are shown in Fig. 1. Distributions representing Hauser-Feshbach calculations with (dashed lines) as well as without (solid lines) width fluctuation corrections are illustrated. The agreements between the calculated and experimental elastic angular distributions are good. It is clear that optical potential parameters obtained from the search procedure for Cr, Fe and Ni are useful for extrapolation purposes to lower neutron energies. However, the fact that the agreements between the experimental and calculated differential cross sections (corrected for level-width fluctuations) are better at 2.52 and 2.76 MeV than at lower energies is probably fortuitous. One explanation is that in spite of the comparatively large energy spread ($\pm$ 50 keV) in the neutron beam the resonance effects are not smoothed out and the statistical assumptions of the optical model are not completely satisfied experimentally. This explanation is confirmed by the results obtained from five parameter searches on Cr, Fe and Ni at 3 MeV. In the latter case the optical model parameters obtained differed somewhat from the mean values applied in calculations at lower energies, but appreciably better agreements

were obtained between experiment and theory even without Moldauer corrections. Lister and Smith [7] have shown that cross sections for elastic and inelastic neutron scattering measured in the energy range 0.3 to 1.5 MeV for even mass number germanium isotopes tended to be reasonably well described in terms of the Hauser-Feshbach statistical model without corrections for level-width fluctuations. Furthermore they found that the agreement between measured and calculated inelastic cross sections could be appreciably improved with a model properly accounting for vibrational effects. Also for the elements Cr, Fe and Ni consisting mainly of even mass number isotopes (9.5 per cent Cr^{53} can be neglected) it is likely that the differential elastic cross sections are influenced by collective effects. There is a strong excitation of the 2+ state by inelastic nucleon scattering and it is possible that the coupling to this state is sufficiently strong to allow its virtual excitation to have an observable effect on the elastic scattering from even nuclei. These facts also demonstrate some of the difficulties in testing the usefulness of the Moldauer level-width theory.

With the exception of the real potential depth U, the optimum parameter values of V (Table II) from the five-parameter analyses are essentially independent of the neutron energy. However, the variations of U seem to be coupled to variations of r_{oU}, so that the well known Ur_{oU}^2 ambiguity is fulfilled.

For the predominantly even mass number nuclei Cr, Fe and Ni (Tables III to V) the real potential depth decreases slowly with the neutron energy. The parameters r_{oU}, r_{oW}, a and W are generally independent of energy.

Satisfactory agreement has been obtained between the optical model total cross sections and the experimental ones given by Foster [8], Galloway [9] and those compiled by Schmidt [10].

---

[7] Lister, D. and Smith, A. B., Fast-neutron scattering from germanium. Phys. Rev. 183 (1969) 954.

[8] Foster, D.G. Jr. and Glasgow, D. W. in Neutron cross sections. 1965 - 1966. 2nd ed. Suppl. 2. (BNL-325).

[9] Galloway, L. A. and Shrader, E. F., Neutron total cross section measurements using a "white" neutron source. 1966. (COO-1573-6).

[10] Schmidt, J. J., Neutron cross sections for fast reactor materials. Part 3: Graphs. 1962. (KFK-120).

TABLE I. The experimental parameters characteristic of the elastic scattering cross section measurements.

Neutron source	$T(p, n)He^3$ for $E_n \leq 4.6$ MeV $D(d, n)He^3$ for $E_n > 4.6$ MeV
Gas target	Length of gas target cell 3 cm Nickel foil thickness 2.5 mg/cm^2 Gas pressure in the cell 1 kp/cm^2 (for T_2 as well as for D_2) Total energy spread $\pm$ 50 keV for $E_n \leq 4.6$ MeV Total energy spread $\pm$ 90 keV for $E_n > 4.6$ MeV
Accelerator beam	Beam pulse frequency 1 MHz Beam pulse width at half-height 2 ns Mean target current 1.5 μA
Sample size and purity	V to Ni, cylinders having lengths of 5.0 cm, 0.95 cm inner diameter and 2.5 cm outer diameter Polythene scatterer, 3.0 cm in length, 0.95 cm outer diameter and 0.65 cm inner diameter Sample purity $\geq$ 99.5 %
Target-scatterer-detector distances	Target-scatterer 10 cm Scatterer-detector 300 cm
Neutron time-of-flight detector	Scintillator NE102A, size 10 cm diameter and 5 cm length Spectrometer time resolution 3 ns
Neutron flux measurements	The neutron flux was monitored with a directional long counter
Angular interval	The angular distributions have been measured in the angular region 20° to 160° in 10° steps except in the foreward directions, where measurements were performed in 5° step
Background conditions	The signal-to-background ratio at the position of the eleastic peak was 7 to 1 in the most unfavourable case i.e. at 8 MeV neutron energy and at the forward scattering angles, but was much more favourable at lower energies
Counting statistics	Statistical errors for the number of counts in the elastic peaks of the time-of-flight spectra $\leq$ 2 % Statistical error for the number of monitor counts 0.3 %
Errors	The experimental cross section errors are 5 per cent except for Cr below 2.5 MeV and for Fe and Ni below 3 MeV, where the errors are about 10 per cent

TABLES II to V. Optimum values of the optical potential parameters from five-parameter analyses of V, Cr, Fe and Ni. The total elastic cross sections σ_{el} and the total cross sections σ_T calculated with the optical potential are also included, together with the corresponding experimental quantities σ_{el}^{exp} and σ_T^{exp}. The compound elastic cross sections σ_{ce} have been calculated with the Hauser-Feshbach formalism.

TABLE II. Vanadium

E_n (MeV)	2.47	3.00	3.49	4.00	4.56	5.50	6.09	7.05	8.05
U (MeV)	51.3	47.4	48.6	48.1	49.2	52.3	51.8	50.7	46.6
W (MeV)	8.40	8.40	8.41	8.30	8.12	7.90	7.94	7.94	6.43
r_{oU} (fm)	1.19	1.26	1.24	1.25	1.23	1.19	1.19	1.21	1.23
r_{oW} (fm)	1.21	1.23	1.22	1.21	1.18	1.17	1.20	1.20	1.25
a (fm)	0.65	0.66	0.66	0.66	0.65	0.65	0.66	0.64	0.65
σ_T (b)	3.58	3.81	3.71	3.70	3.60	3.37	3.28	3.24	3.10
σ_{se} (b)	1.79	2.08	2.11	2.19	2.19	2.08	2.01	1.96	1.85
σ_A (b)	1.79	1.73	1.60	1.51	1.41	1.29	1.27	1.28	1.25
σ_{ce} (b)	0.67	0.60	0.31	0.23	0.17	0	0	0	0
σ_{el} (b)	2.46	2.68	2.42	2.42	2.36	2.08	2.01	1.96	1.85
σ_{el}^{exp} (b)	2.45±0.15	2.66±0.16	2.49±0.15	2.61±0.15	2.40±0.14	2.05±0.12	2.00±0.12	1.96±0.12	1.85±0.11
σ_T^{exp} (b)	3.92±0.14 [Ref. 8]	3.77±0.09 [Ref. 8]	3.75±0.07 [Ref. 8]	3.83±0.07 [Ref. 8]	3.74±0.06 [Ref. 8]	3.64±0.07 [Ref. 8]	3.51±0.07 [Ref. 8]	3.32±0.07 [Ref. 8]	3.14±0.08 [Ref. 8]
	3.67±0.04 [Ref. 9]	3.75±0.04 [Ref. 9]	3.75±0.04 [Ref. 9]	3.75±0.04 [Ref. 9]	3.75±0.04 [Ref. 9]	3.75±0.04 [Ref. 9]	3.50±0.04 [Ref. 9]	3.45±0.03 [Ref. 9]	3.25±0.03 [Ref. 9]

TABLE III. Chromium

E_n (MeV)	2.47	3.00	3.49	4.00	4.56	5.50	6.09	7.05	8.05
U (MeV)	55.4	50.9	51.4	50.2	49.7	51.7	49.7	48.0	50.6
W (MeV)	8.81	8.33	8.45	8.15	7.49	8.74	9.49	9.77	9.13
r_{oU} (fm)	1.11	1.19	1.17	1.21	1.20	1.19	1.21	1.24	1.21
r_{oW} (fm)	1.15	1.15	1.20	1.16	1.25	1.18	1.15	1.23	1.21
a (fm)	0.63	0.66	0.64	0.66	0.65	0.68	0.68	0.64	0.61
σ_T (b)	3.34	3.69	3.53	3.62	3.68	3.42	3.41	3.27	3.07
σ_{se} (b)	1.66	2.00	1.99	2.15	2.34	2.03	1.99	1.85	1.76
σ_A (b)	1.68	1.69	1.54	1.47	1.34	1.39	1.42	1.42	1.31
σ_{ce} (b)	0.74	0.49	0.28	0.17	0.10	0	0	0	0
σ_{el} (b)	2.40	2.49	2.27	2.32	2.44	2.03	1.99	1.85	1.76
σ_{el}^{exp} (b)	2.39±0.12	2.50±0.13	2.24±0.11	2.21±0.11	2.44±0.12	1.99±0.10	2.00±0.10	1.83±0.09	1.78±0.09
σ_T^{exp} (b)	3.45±0.12 [Ref. 8]	3.49±0.07 [Ref. 8]	3.80±0.08 [Ref. 8]	3.75±0.06 [Ref. 8]	3.75±0.06 [Ref. 8]	3.66±0.07 [Ref. 8]	3.66±0.08 [Ref. 8]	3.38±0.08 [Ref. 8]	3.19±0.08 [Ref. 8]

TABLE IV. Iron

E_n (MeV)	2.96	3.95	4.56	7.05	8.05
U (MeV)	51.1	53.8	49.2	46.7	49.3
W (MeV)	10.8	9.84	11.19	10.46	10.45
r_{oU} (fm)	1.21	1.16	1.24	1.24	1.23
r_{oW} (fm)	1.15	1.05	1.16	1.24	1.20
a (fm)	0.61	0.63	0.61	0.66	0.64
σ_T (b)	3.34	3.45	3.43	3.36	3.32
σ_{se} (b)	1.68	1.97	1.89	1.85	1.85
σ_A (b)	1.66	1.48	1.54	1.51	1.47
σ_{ce} (b)	0.38	0.13	0.09	0	0
σ_{el} (b)	2.06	2.10	1.98	1.85	1.85
σ_{el}^{exp} (b)	2.14±0.11	2.08±0.10	2.10±0.11	1.80±0.09	1.76±0.09
σ_T^{exp} (b)	3.40+0.07 [Ref. 8]	3.68+0.07 [Ref. 8]	3.67+0.07 [Ref. 8]	3.65+0.09 [Ref. 8]	3.31+0.09 [Ref. 8]

TABLE V. Nickel

E_n (MeV)	3.00	3.49	4.00	4.56	6.09	7.05	8.05
U (MeV)	53.2	54.1	53.4	50.0	48.5	51.5	45.7
W (MeV)	8.68	8.37	8.77	10.09	10.07	11.3	9.10
r_{oU} (fm)	1.18	1.14	1.15	1.17	1.21	1.18	1.25
r_{oW} (fm)	1.22	1.11	1.16	1.15	1.20	1.18	1.29
a (fm)	0.64	0.66	0.67	0.72	0.73	0.71	0.68
σ_T (b)	3.27	3.38	3.36	3.60	3.68	3.45	3.59
σ_{se} (b)	1.70	1.87	1.88	1.99	2.04	1.86	2.01
σ_A (b)	1.57	1.51	1.48	1.61	1.64	1.59	1.58
σ_{ce} (b)	0.41	0.23	0.12	0.09	0	0	0
σ_{el} (b)	2.11	2.10	2.00	2.08	2.04	1.86	2.01
σ_{el}^{exp} (b)	2.15±0.11	2.06±0.10	2.00±0.10	2.00±0.10	1.83±0.09	1.79±0.09	1.71±0.09
σ_T^{exp} (b)	3.27±0.08 [Ref. 8]	3.49±0.07 [Ref. 8]	3.51±0.06 [Ref. 8]	3.63±0.06 [Ref. 8]	3.74±0.07 [Ref. 8]	3.57±0.08 [Ref. 8]	3.53±0.08 [Ref. 8]

TABLES VI to VIII Cross sections and extrapolated values of the optical potential parameters of Cr, Fe and Ni. σ_T, σ_{se} and σ_A are the total cross section, the total shape elastic cross section and the total absorption cross section. σ_{ce}^{corr} and σ_{ce}^{HF} are the total compound elastic cross sections with and without level-width fluctuation corrections, respectively. σ_{el}^{corr} and σ_{el}^{HF} are the corresponding total elastic cross sections.

TABLE VI. Chromium

E_n (MeV)	1.77	2.02	2.27	2.76
U (MeV)	52.9	52.7	52.5	52.2
W (MeV)	8.70	8.70	8.70	8.70
r_{oU} (fm)	1.19	1.19	1.19	1.19
r_{oW} (fm)	1.19	1.19	1.19	1.19
a (fm)	0.65	0.65	0.65	0.65
σ_T (b)	3.43	3.45	3.47	3.51
σ_{se} (b)	1.45	1.54	1.63	1.80
σ_A (b)	1.98	1.91	1.84	1.71
σ_{ce}^{HF} (b)	1.11	1.02	0.82	0.58
σ_{ce}^{corr} (b)	1.40	1.30	1.12	0.84
σ_{el}^{HF} (b)	2.56	2.56	2.45	2.38
σ_{el}^{corr} (b)	2.85	2.84	2.75	2.64
σ_{el}^{exp} (b)	2.31±0.20	2.46±0.25	2.49±0.23	2.55±0.26
σ_T^{exp} (b)	3.25±0.33 [Ref. 10]	3.70±0.37 [Ref. 10]	3.20±0.32 [Ref. 10]	3.74±0.18 [Ref. 10]

TABLE VII. Iron

E_n (MeV)	1.77	2.02	2.27	2.52	2.76
U (MeV)	52.9	52.7	52.5	52.3	52.1
W (MeV)	10.55	10.55	10.55	10.55	10.55
r_{oU} (fm)	1.20	1.20	1.20	1.20	1.20
r_{oW} (fm)	1.16	1.16	1.16	1.16	1.16
a (fm)	0.63	0.63	0.63	0.63	0.63
σ_T (b)	3.33	3.31	3.31	3.31	3.32
σ_{se} (b)	1.40	1.44	1.50	1.56	1.61
σ_A (b)	1.93	1.87	1.81	1.75	1.71
σ_{ce}^{HF} (b)	0.79	0.69	0.62	0.55	0.46
σ_{ce}^{corr} (b)	1.09	0.98	0.88	0.79	0.68
σ_{el}^{HF} (b)	2.19	2.13	2.12	2.11	2.07
σ_{el}^{corr} (b)	2.49	2.42	2.38	2.35	2.29
σ_{el}^{exp} (b)	1.88±0.19	2.13±0.21	1.85±0.19	2.49±0.25	2.36±0.25
σ_T^{exp} (b)	2.85±0.14 [Ref. 10]	3.20±0.16 [Ref. 10]	3.20±0.16 [Ref. 10]	3.90±0.04 [Ref. 9]	3.25±0.04 [Ref. 9]

TABLE VIII. Nickel

E_n (MeV)	1.77	2.02	2.27	2.52	2.76
U (MeV)	55.9	55.5	55.1	54.8	54.3
W (MeV)	9.32	9.32	9.32	9.32	9.32
r_{oU} (fm)	1.19	1.19	1.19	1.19	1.19
r_{oW} (fm)	1.20	1.20	1.20	1.20	1.20
a (fm)	0.69	0.69	0.69	0.69	0.69
σ_T (b)	3.20	3.15	3.12	3.12	3.15
σ_{se} (b)	1.38	1.36	1.37	1.41	1.47
σ_A (b)	1.82	1.79	1.75	1.71	1.68
σ_{ce}^{HF} (b)	1.08	0.89	0.74	0.54	0.46
σ_{ce}^{corr} (b)	1.36	1.19	1.04	0.90	0.77
σ_{el}^{HF} (b)	2.46	2.25	2.11	1.95	1.93
σ_{el}^{corr} (b)	2.74	2.55	2.41	2.31	2.24
σ_{el}^{exp} (b)	2.23±0.22	2.20±0.22	2.37±0.24	2.36±0.24	2.35±0.24
σ_T^{exp} (b)	3.22±0.16 [Ref. 10]	3.20±0.16 [Ref. 10]	3.21±0.32 [Ref. 10]	3.22±0.16 [Ref. 10]	3.23±0.16 [Ref. 10]

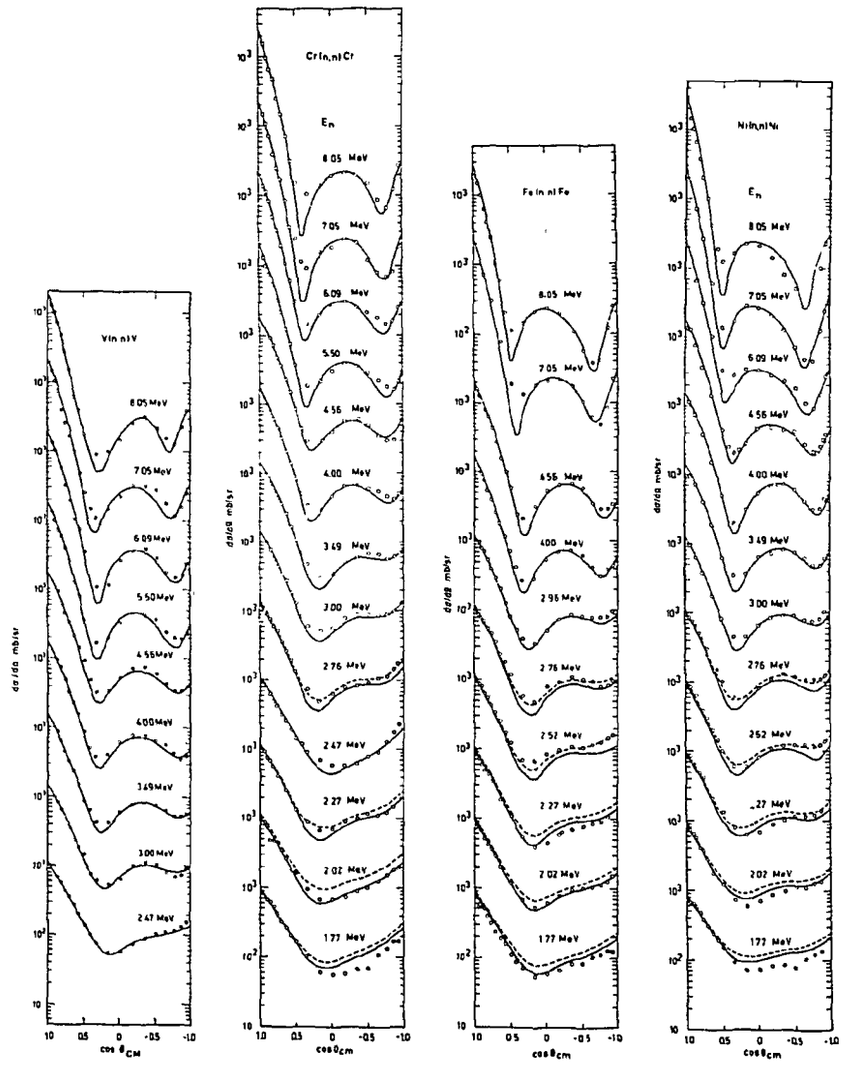

Fig. 1 The experimental differential elastic scattering cross sections of V, Cr, Fe and Ni (circles). The solid lines represent optical model calculations which take no account of width fluctuations and the dashed lines represent those with width fluctuation corrections included.

I.1.3. Investigation of the effects of sample size in neutron scattering measurements

E. Almén, M.A. Etemad *, B. Holmqvist
P.I. Johansson and T. Wiedling
Atomic Energy Company, Studsvik, Nyköping

Fast neutron elastic and inelastic scattering cross sections are usually measured relative to a standard cross section with well known properties. Thus the precision of the measurement will depend upon the knowledge of the standard cross section which must be known with an appreciably higher accuracy than that to be determined in order to give a negligable contribution to the total error. The size of the scattering sample may influence the accuracy of the measurement. This effect has been studied in a recent, preliminary n-p scattering expreriment using a time-of-flight arrangement with a plastic scintillation neutron detector. The measurements were run with polythene scatterers, one of length 3.0 cm, 0.95 cm outer diameter and 0.65 cm inner diameter and the other of length 2.0 cm, 0.40 cm outer diameter and 0.20 cm inner diameter. The energy of the incident neutrons was 6.0 MeV and the total energy spread $\pm$ 100 keV. The intensities of scattered neutrons were observed at several angles between 24° and 55° corresponding to an energy interval from 5.0 to 2.0 MeV. The preliminary results show that the energy resolution obtained with the small scatterer is about 10 per cent being almost independent of the neutron energy throughout the interval. For the large scatterer the energy resolution is about 10 per cent at 5 MeV rising roughly in a linear way up to 25 per cent at 2 MeV. This shows as expected that it is essential to use a very small polythene sample to get a good energy resolution at low neutron energies. The slopes of the efficiency curves obtained with the two polythene scatterers agree within the accuracy of the measurements.

A similar experiment is also in progress to investigate the effects of the sample size in a neutron elastic scattering cross section experiment. Two iron samples have been used one with the same

---

* On leave from Tehran University Nuclear Centre, Tehran, Iran.

dimensions as the "standard" polythene sample, i.e. length 3.0 cm, inner diameter 0.65 and outer diameter 0.95 cm and the other of length 5.0 cm, inner diameter 0.96 cm and outer diameter 2.5 cm. The measurements were performed with an incident neutron energy of 6 MeV and the total energy spread $\pm$ 100 keV. The scattered neutrons were observed at 14 angles between 20° and 150°.

I.1.4. Gamma-rays from inelastic scattering in nitrogen

H. Condé, B. Lundberg and L.G. Strömberg
Research Institute of National Defence, Stockholm

G. Nyström
Department of Nuclear Physics, University of Lund, Lund

Differential gamma-ray production cross-sections for nitrogen have been measured at incident neutron energies of 4.5, 6 and 7 MeV at an angle of 55 degrees. Time-of-flight techniques were used to suppress the background from neutron interactions in the 17 ccm Ge(Li) detector. The efficiency of this detector was determined by using calibrated γ-sources. The incident neutron flux monitor was calibrated with a proton-recoil telescope counter.

Pronounced gamma lines were observed at 0.730, 1.637, 2.135 and 5.104 MeV.

For the angular distribution measurements at 7 MeV a 25.5 ccm Ge(Li) detector was used together with larger samples to increase the counting rate. Data were taken over the angular range 37° to 142°, laboratory angles.

Data handling has been delayed due to difficulties with computer codes involved.

I.1.5. Gamma-rays from inelastic neutron scattering in oxygen

B. Lundberg, L.G. Strömberg and H. Condé
Research Institute of National Defence, Stockholm

The differential cross-section for the production of the 6.13 MeV gamma-ray from the $^{16}O(n, n'\gamma)$ reaction has been measured between the reaction threshold and 8.2 MeV. The gamma-rays were detected with a large NaI(Tl) crystal using time-of-flight techniques. Angular distributions have been studied at two resonance energies in the cross-section, viz. 6.87 and 7.82 MeV. Spins for the involved levels in the compound nucleus are proposed and the shapes of the angular distributions are compared with calculations based on the compound nucleus model. The results are also compared with previously reported measurements.

I.1.6. Gamma-ray lines from (n, 2n) and (n, n') reactions in radiogenic and natural lead

Bodil Jönsson
Department of Physics, Lund University, Lund

Discrete γ-ray lines emitted after (n, 2n) and (n, n') reactions in radiogenic and natural lead at 15.5 MeV neutron energy have been studied. Differential 120° cross sections have been determined relative to the cross section for the ground state transition from the 4.44 MeV level of ^{12}C populated through inelastic scattering. The (n, 2n) and (n, n') contributions to the cross sections for the most dominant γ-ray lines in ^{206}Pb and ^{207}Pb have been separated. Upper and lower limits of the cross sections for (n, 2n) and (n, n') reactions in lead are estimated. The results indicate that the statistical theory of nuclear reactions fails to give a correct description of neutron emission processes in lead at 15 MeV neutron energy.

I.1.7. Fast neutron inelastic scattering in the energy range 2 to 4.5 MeV

E. Almén, M.A. Etemad*,
B. Holmqvist and T. Wiedling
Atomic Energy Company, Studsvik, Nyköping

These investigations have been made in order to collect information on neutron inelastic cross sections for reactor physics purposes as well as for a systematic study of nuclear models describing the neutron inelastic scattering mechanism.

Up to now measurements have been made in the energy range 2 to 4.5 MeV for the following natural elements: Be, Mg, Al, S, Ti, V, Cr, Mn, Fe, Co, Ni, Cu, Zn, Ga, Nb, In, Ta, Pb, Pb_r (radiogenic lead) and Bi in energy steps of roughly 0.25 MeV. The experiments were performed with a time-of-flight spectrometer having a detector consisting of a fast plastic scintillator viewed by a photomultiplier. This equipment has been described elsewhere [1]. The measurements have been made only at one angle, 125°. This is sufficient with regard to the angular distribution functions, which are usually either isotropic or only sligthly anisotropic. The total inelastic cross section is just 4π times the measured differential cross section when the angular distribution function is of the simple form $a_o + a_2P_2(\cos\theta)$ a function which is a good approximation to many inelastic angular distrubutions.

The cross sections were measured relative to those of the n-p reaction by observing neutron scattering from hydrogen. The n-p scattering process was also used for the dctermination of the relative neutron detector efficiency as described in reference [1].

The analyses of the data have at present only been completed for six elements, i.e. Al, V, Mn, Fe, Nb, and Bi.

---

* On leave from Tehran University Nuclear Center, Tehran, IRAN

[1] Holmqvist, B., A systematic study of fast neutron elastic scattering in the energy region 1.5 to 8.1 MeV. Arkiv Fysik 38 (1968) 403.

The experimental cross sections have been corrected for flux attenuation, multiple scattering and finite geometry of target - scatterer system using a Monte Carlo technique.

The excitation functions corresponding to inelastic transitions have been compared with cross sections calculated with the Hauser and Feshbach (H. F.) statistical model corrected for level width fluctations. The transmission coefficients necessary for the H. F. calculations were obtained from interpolations and extrapolations using the optical model potential parameters given in reference [2]. Information on level energies, spins and parities was obtained from various references mentioned elsewhere [3]. When no information concerning spins and parities was available, cross sections for those levels were calculated with estimated spins and parities.

The results have been plotted in Fig. 1 where the circles represent the experimental cross sections and the curves the calculated excitation functions showing that in some cases the H. F. cross sections are systematically too large.

---

[2] Holmqvist, B. and Wiedling, T., Neutron elastic scattering cross sections, experimental data and optical model cross section calculations. 1969 (AE-366).

[3] Almén, E. et. al., Fast neutron inelastic scattering in the energy range 2 to 4.5 MeV. Nuclear Data for Reactors (Proc. Conf. Helsinki, 1970) II, IAEA, Vienna (1970) 349.

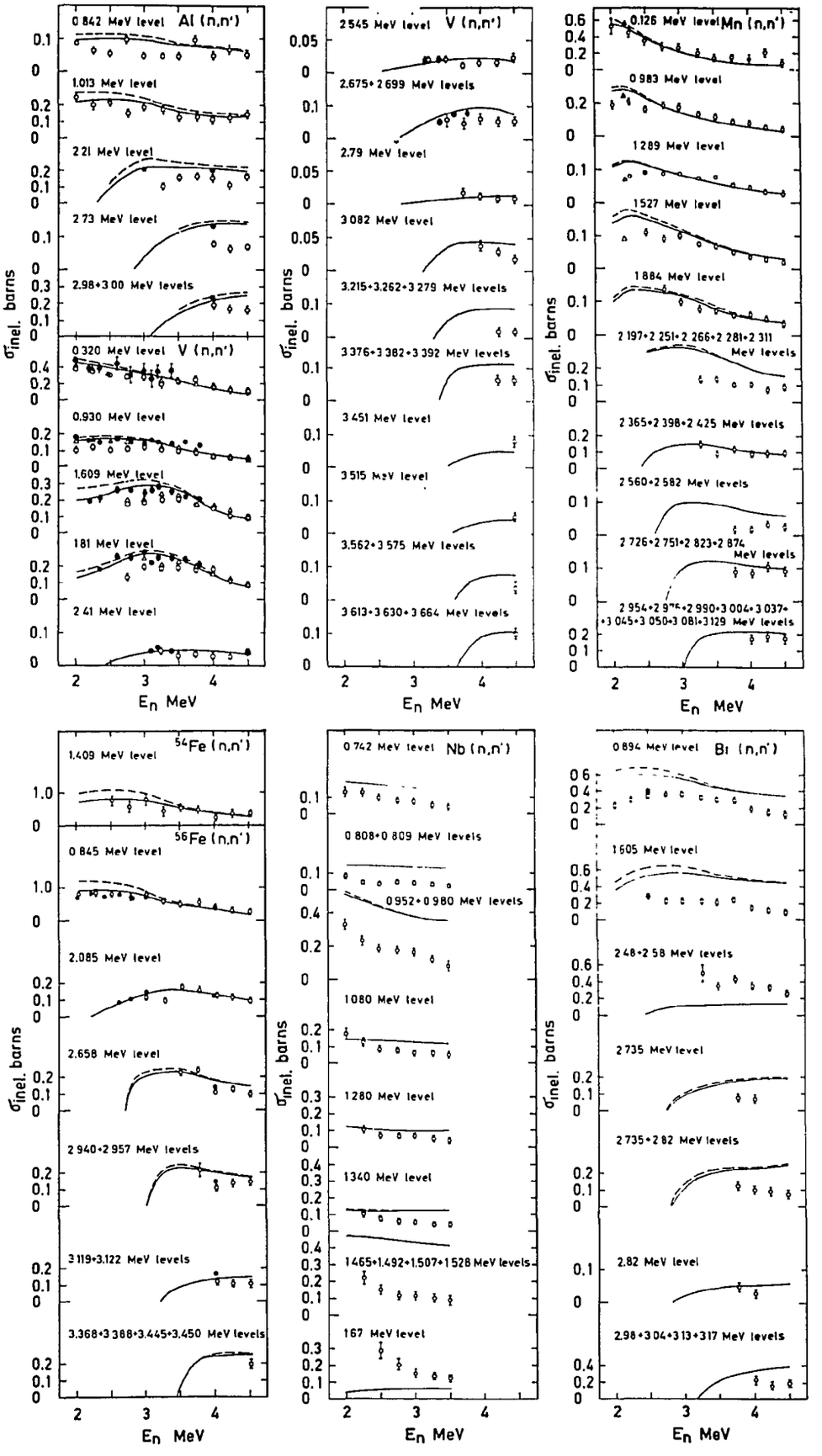

Fig. 1 Excitation functions for inelastic neutron scattering from the elements Al, V, Mn, Fe, Nb and Bi. The experimental results (circles) are compared with cross sections calculated from the H. F. formalism (dashed lines) as well as with H. F. cross sections corrected for Moldauer level width fluctuation (solid lines). The filled circles refer to results compiled in reference [3].

I.2. FISSION PHYSICS

I.2.1. Studies of the fission threshold structure for ^{232}Th, ^{231}Pa and ^{227}Ac

M. Holmberg and L-E Persson
Research Institute of National Defence, Stockholm

Measurements of the fission cross section and of the angular distributions of the fission fragments have been made for ^{232}Th and ^{231}Pa. The "Makrofol" technique is used in the measurements of the angular distributions. The results are not yet analyzed.

I.2.2. Prompt $\bar{\nu}$ in spontaneous and neutron induced fission of ^{236}U

H. Condé and M. Holmberg
Research Institute of National Defence, Stockholm

The energy dependence of prompt $\bar{\nu}$ has been investigated for the neutron induced fission of ^{236}U in the energy range 0.8 - 6.7 MeV. The fission neutron detector was a large liquid scintillator. The present data can be fitted with a straight line $\bar{\nu}_p(E_n) = 2.316 + 0.131\ E_n$. Prompt $\bar{\nu}$ for the spontaneous fission of ^{236}U and ^{238}U were also measured with the result $\bar{\nu}_p(^{236}U) = 1.90 \pm 0.05$ and $\bar{\nu}_p(^{238}U) = 2.00 \pm \pm 0.05$. The ratio between the half-lives for spontaneous fission of ^{238}U and ^{236}U was determined to be 0.30 ± 0.03.

I.2.3. Variation in prompt pulse efficiency for two liquid scintillator tanks used in $\bar{\nu}$-measurements at FOA

H. Condé, J. Hansén and L. Widén
Research Institute of National Defence, Stockholm

A measurement of the variation in prompt pulse efficiency versus number of fission neutrons has been performed for two different liquid scintillator tanks used in $\bar{\nu}$-measurements at FOA, Stockholm. The results have been used to calculate a correction to the absolute $\bar{\nu}$-value of ^{252}Cf measured by Asplund-Nilsson, Condé and Starfelt. A correction of 0.6 % was obtained. The corrected prompt $\bar{\nu}$-value for the spontaneous fission of ^{252}Cf is 3.776 ± 0.034.

I.2.4. Neutron energy spectra from neutron induced fission of ^{238}U and of ^{235}U

E. Almén, B. Holmqvist and T. Wiedling
Atomic Energy Company, Studsvik, Nyköping

The intensity distributions of neutron fission spectra are of primary importance in nuclear reactors in connection with their influence on the reactivity. Therefore accurate knowledge of the shapes of neutron fission spectra are of interest in reactor physics calculations. The results from previously reported measurements of the neutron spectra from different fissile isotopes show that, in spite of the relatively small quoted errors in the individual measurements, there is rather large spread among the results indicating large systematic uncertainties. For this reason time-of-flight measurements of the neutron spectra of some fissile isotopes at fast incident neutron energies are in progress at our laboratory. Up to now the fission neutron spectra from ^{238}U have been studied at 1.35 and 2.02 MeV incident neutron energy and that from ^{235}U at 0.945 MeV. The 0.945 and 1.35 MeV measurements were performed with the detector positioned at an angle of 90° relative to the incident neutron beam but at 2.02 MeV three detector angles, i.e. 40°, 90° and 150°, were chosen in order to observe whether there were any systematic deviations due to angle dependent effects.

The fission neutron spectra have been analyzed in the energy ranges 0.95 to 9.5 MeV, 1.5 to 8.0 MeV and 2.1 to 11.0 MeV at incident neutron energies of 0.945, 1.35 and 2.02 MeV, respectively. Below these energies there are unresolved peaks from elastic and inelastic neutron scattering superposed on the fission neutron spectrum making the analysis of the latter difficult and uncertain.

An accurate knowledge of the neutron detector response function as well as the energy calibration of the spectrometer is required to determine neutron intensities from a fission spectrum over a large dynamic range. However, it is sufficient for the determination of the shape of the neutron spectrum to measure the relative efficiency of the detector. This has been done by measuring scattering from hydrogen at different angles and at different primary neutron energies

using a polythene sample. The energy calibration of the time- of-flight spectrometer was performed by observing the positions of peaks corresponding to elastic and inelastic neutron scattering from a large number of elements as well as the position of the gamma ray peak.

Corrections for flux attenuation in the uranium and the polythene samples have been calculated using Monte Carlo techniques and have been applied to the experimental results.

A Maxwellian distribution $N(E) \sim E^{1/2} \exp(-E/T)$ has been fitted to the experimental neutron fission spectra (N(E) is the intensity of the fission neutrons having the energy E). A semi-logarithmic presentation of the fission neutron spectra obtained in the present investigations is given in Fig. 1 showing that the Maxwellian distribution describes the experiments well within the analyzed energy ranges. The values of the parameter T, the Maxwellian temperature, have been obtained by least squares fit procedures. For ^{238}U a temperature of 1.29 ± 0.03 MeV was obtained at 1.35 MeV incident neutron energy. The fission neutron spectra from the same isotope observed at angles of 40°, 90° and 150° at 2.02 MeV give the individual temperature values 1.28 ± 0.02, 1.28 ± 0.02 and 1.30 ± 0.02 MeV, respectively, indicating that there are no significant angle dependent effects. The mean value of the three measurements is 1.29 ± 0.02 MeV. A value of 1.27 ± 0.01 MeV of the Maxwellian temperature gives the best fit to the experimental fission neutron spectrum from ^{235}U at an incident neutron energy of 0.945 MeV.

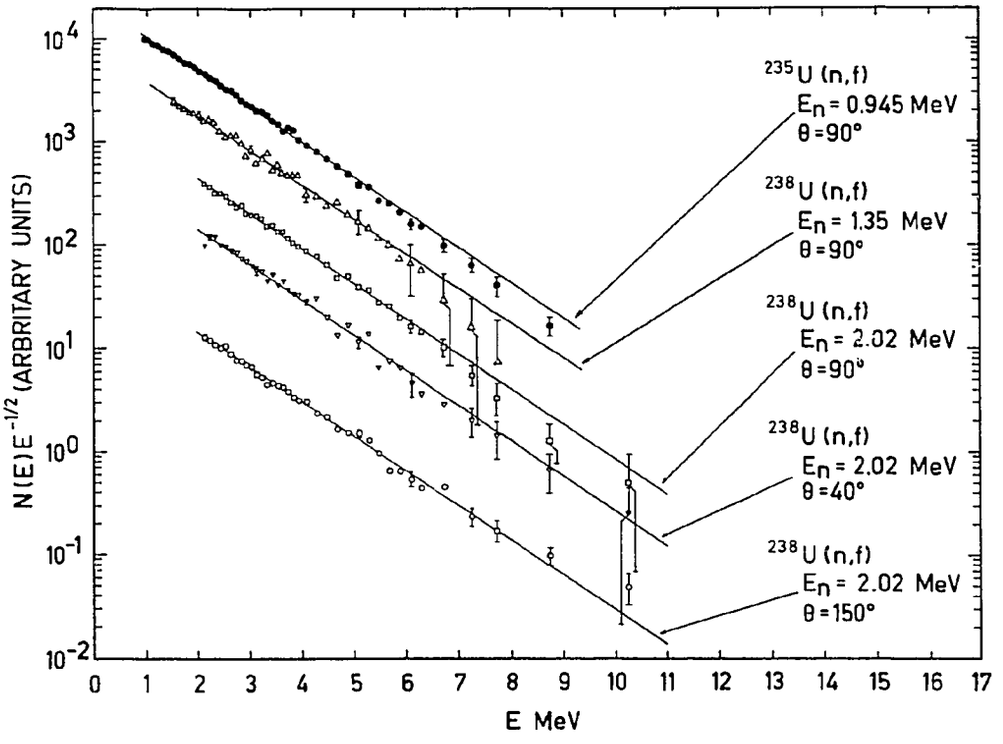

Fig. 1 The fission neutron spectra of ^{235}U recorded at 0.945 MeV incident neutron energy and of ^{238}U obtained at 1.35 and 2.02 MeV primary energies. The lines represents least squares fits to the experimental points assuming Maxwellian temperature distributions.

I.3. NEUTRON CAPTURE

I.3.1. Fast neutron capture cross section studies

J. Hellström, R. Johnson, S. Malmskog and S. Beshai
Atomic Energy Company, Studsvik, Nyköping

A large liquid scintillator detector has been designed to be used in (n, γ) cross section measurements in the 100 keV region and to operate according to the Moxon-Rae principle. Eight photomultipliers view different layers of the scintillator volume and by demanding coincidences between pairs of the photomultipliers the Moxon-Rae condition is fullfilled. It is obvious that such a system used in combination with time-of-flight techniques will be both complicated and expensive if the coincidences were to be recorded for each pair of photomultipliers separately. Another solution, "cablemates", which is both simpler, cheap and offers some other advantages has thus been developed.

Instead of recording coincidences between pairs of photomultipliers in separate electronic systems the coincidences related to a certain pair of photomultipliers are being distinguished from one another with the help of a delay cable arrangement. Thus the same electronics needed for one pair of photomultipliers can be used for all of them. The principle of the system is shown in Fig. 1 where also a typical TAC spectrum from a radioactive source is shown. Also indicated are the locations of the coincidences between different photomultipliers.

Two major advantages are obvious from Fig. 1. First, the coincidences fullfilling the Moxon-Rae condition are all gathered in the peak in the middle of the spectrum and can easily be separated from other coincidences either with help of a single channel analyzer or by selecting an appropriate time range of the time-to-pulse height converter. Second, other coincidences than those fullfilling the Moxon-Rae condition can automatically be recorded.

The set up described has been tested with different radioactive sources having different decay modes and has been found to work satisfactorily.

Next, time-of-flight techniques were employed together with the above described system. In this connection two different solutions have been tried. The first splits up the pulse generated by the ac-

celerator beam in four different pulses each being delayed to match the time relations between the Moxon-Rae pulses. This is shown in Fig. 2.

The time range of the second time to pulse height converter, i. e. the time-of-flight spectrum, is in this case limited by the delay cables connected to the machine generated pulse and the photomultipliers and should be chosen to be less than t (= the time difference between two pairs of phothomultipliers Fig. 2). This system can be most advantageously used in an experiment where thin targets are used. However, in experiments where thick targets are used, i. e. when capture events initiated by neutrons of energies ranging over a rather long time spectrum are to be recorded, another solution has been tried. In the latter case the machine pulse is not split up but is used directly together with summed pulses from the photomultipliers on one side of the detector to give a normal time-of-flight spectrum which is then gated with the Moxon-Rae pulses. Contrary to the previous case only the repetition rate of the machine pulses sets the limit of the time range of the time to pulse height converter. The principle for this system is shown in Fig. 3.

It is clear that both time-of-flight spectra and time-of-flight spectra gated with the Moxon-Rae condition can easily be recorded simultaneously in both cases described.

Some preliminary runs have been made to check the different set ups. The reaction $^{19}F(p, \alpha\gamma)$ was used to verify that the systems shown in Figs. 2 and 3 worked in principle. Next, kinematically collimated neutrons from the reaction $^{7}Li(p, n)$ were used to measure (n, γ) cross sections. A series of samples with a large range of different cross sections (Sn(88mb), Mo(140mb), Cd(330mb), Au(515mb), Ta(735mb)) were used. Although these measurements agreed with previously measured cross sections for the samples to within 15 %, it is as yet too early to place any confidence limit on the derived results.

Finally (n, γ) cross sections were measured for Ta and Au using a 30 keV Li-target and maximum neutron energies of approximately 100 keV. The data is currently being analyzed.

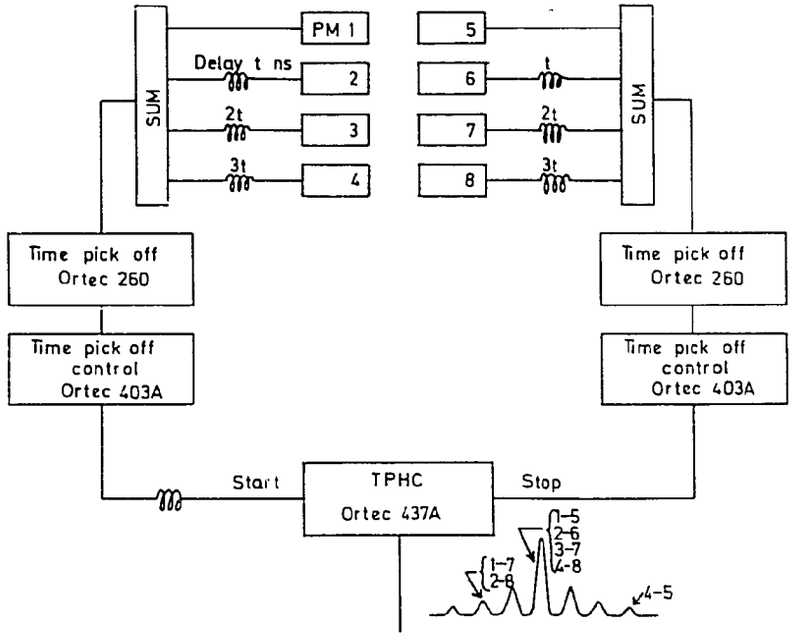

Fig. 1 The principle for distinguishing coincidences related to a certain pair of photomultipliers from other using delay cables. The distribution of some of the coincidences is indicated.

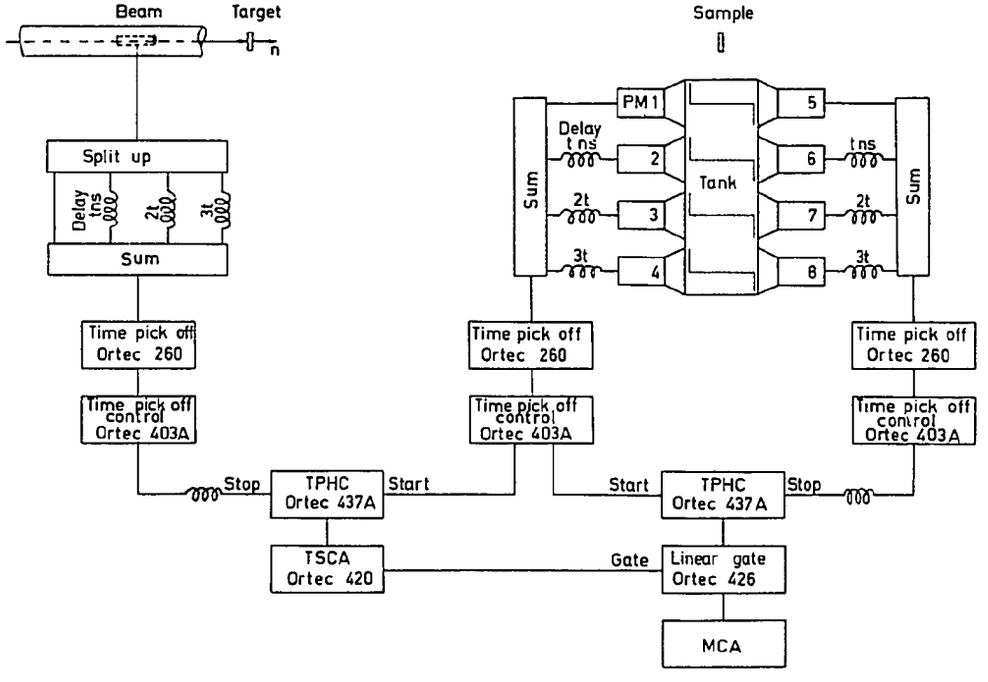

Fig. 2 The system showed in figure 1 together with electronics needed in time-of-flight experiments using a thin neutron target as described in the text.

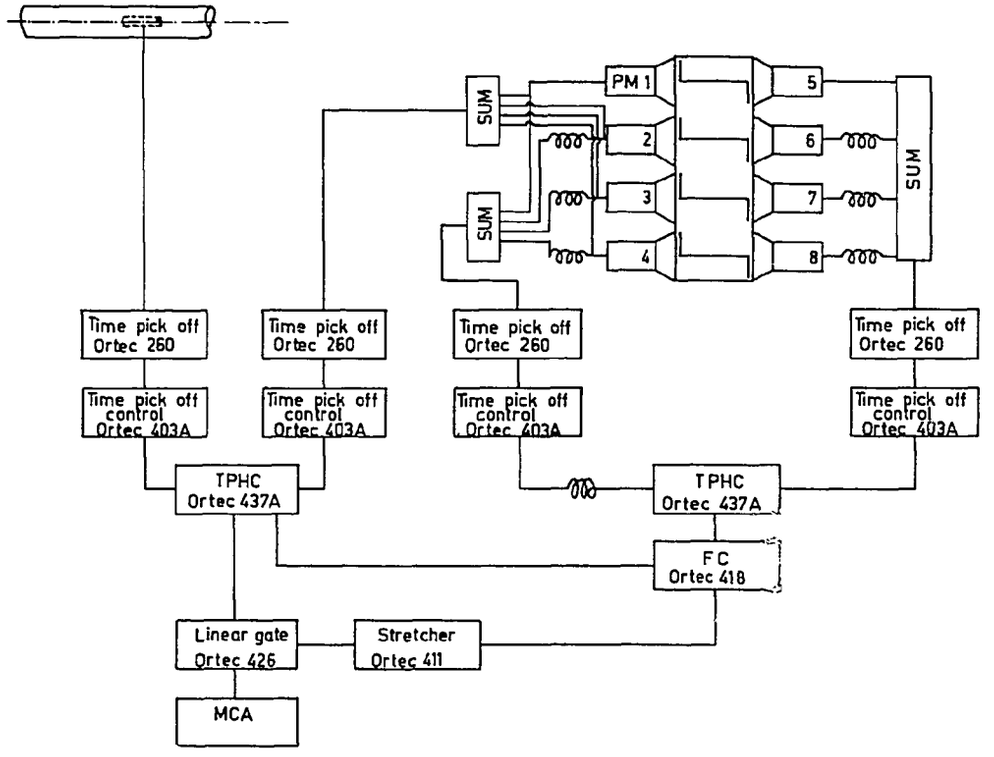

Fig. 3 The electronics to be used in experiments using thick neutron targets where the whole time-of-flight spectrum gated with the Moxon-Rae condition is to be recorded.

I.3.2. Neutron capture cross sections in F, Mg, Al, Si, P and S from 20 to 80 keV

I. Bergqvist and G. Nyström
Department of Physics, University of Lund, Lund

B. Lundberg
Research Institute of National Defence, Stockholm

Neutron radiative capture cross sections have been measured in the energy region 20 to 80 keV using time-of-flight techniques with a 12.7 cm x 10.2 cm NaI(Tl) scintillator. The samples studied were natural samples of F, Mg, Al, Si, P and S. Radiative widths were determined for the resonances at 27 keV (1.4 ± 0.3 eV) and 50 keV (1.5 ± 0.3 eV) in ^{19}F, 84 keV (4.0 ± 0.9 eV) in ^{24}Mg and 35 keV (1.9 ± 0.3 eV) in ^{27}Al. Resonances were also observed at 45 keV in Mg, 38 keV and 68 keV in Si, 27 keV in P and at 30 keV and 42 keV in S.

I.3.3. Studies of fast neutron capture

I. Bergqvist
Department of Physics, University of Lund, Lund

B. Lundberg
Research Institute of National Defence, Stockholm

L. Nilsson
Tandem Accelerator Laboratory, Uppsala

To explain the magnitude of MeV nucleon capture cross sections in medium-weight and heavy nuclei, one is forced to take into account the influence of semi-direct capture processes through the giant dipole resonance. The interaction between the incident nucleon and the target nucleus may excite the latter to its giant dipole resonance while the incident nucleon is captured into a low-lying single-particle orbit. The decay of the giant dipole excitation gives a high-energy gamma-ray transition from the capturing state to a low-lying single-particle state. In a few cases it is possible to study gamma-ray decay to distinct single-particle states. In such cases the comparison with theoretical predictions becomes sufficiently simple to permit definite conclusions concerning the importance of semi-direct capture processes.

Gamma-ray spectra from neutron capture in the energy range 1 to 8.5 MeV were recorded for Si, P, S, Ni, ^{206}Pb and Bi using time-of-flight techniques. The gamma-ray detector is a NaI(Tl) scintillator, 20.8 cm long and 22.6 cm in diameter.

The results for Ni and Bi have been published previously. The cross sections for transitions to low-lying levels in ^{59}Ni and ^{61}Ni are reasonably well accounted for by the semi-direct capture theories, whereas for Bi the agreement is not equally convincing. The latter observation is supported by a similar study of the ^{206}Pb(n,γ)-reaction. The semi-direct capture theories account for only 10 to 20 % of the cross sections at the peak of the giant dipole resonance for transitions to low-lying single-particle states in ^{207}Pb. The semi-direct capture theories predict an enhancement of the direct capture cross sections by a factor of 10 to 15 in the region of the giant dipole reso-

nance, whereas the observed enhancement is about 50. On the other hand, the shapes of the gamma-ray spectra from neutron capture in ^{206}Pb in the MeV region are in agreement with those expected from the semi-direct capture theories.

For the nuclei in the 2s1d shell the preliminary analysis shows strong primary gamma-ray transitions to bound levels with large single-particle strength.

I.3.4. Gamma-rays from neutron capture in Mg, Si, P and S

I. Bergqvist
Department of Physics, University of Lund, Lund

B. Lundberg
Research Institute of National Defence, Stockholm

The gamma-ray spectra from neutron resonance capture in Mg, Si, P and S (natural samples) in the energy range 10 - 75 keV have been recorded. The gamma-ray spectrometer was a NaI(Tl) crystal, 20.8 cm long and 22.6 cm in diameter. Time-of-flight techniques were used. The gamma-ray spectra were found to be dominated by a few intense gamma-ray lines through low-lying levels in agreement with previous observations. Branching ratios were calculated for the dominating primary lines.

I.3.5. Measurements of conversion electrons and gamma-rays from (n_{th}, γ)-reactions

A. Bäcklin, B. Fogelberg and G. Hedin
The Swedish Research Councils' Laboratory, Studsvik, Nyköping

The conversion electron studies of thermal neutron capture reactions leading to even-even nuclei have continued at the R2 reactor in Studsvik. Results are as follows:

a) ^{156}Gd

The complex electron and gamma ray spectra from this nucleus have now been analyzed and an energy level diagram has been constructed. Members of 21 rotational bands have been found at excitation energies between 1.0 and 2.2 MeV.

b) ^{158}Gd

Work on the establishment of energy levels has been started. Six excited rotational bands of presumably collective character have been identified so far. This work, and the preceeding one, are collaborations with groups at Risø, Denmark and Idaho Falls, USA.

c) ^{236}U

Complementary conversion electron measurements on the low energy part of the spectrum have been performed. A special emphasis has been put on a study of the intraband transitions between members of the $K = 2^-$ band based at 688 keV.

d) ^{240}Pu

Measurements of the conversion electron spectrum below 1 MeV have been started.

e) ^{114}Cd

A careful search for the zero-phonon transitions between the members of the two-phonon multiplet has been performed with the $\pi\sqrt{2}$ electron spectrometer.

II. GENERAL NEUTRON PHYSICS

II. 1. Experimental investigations of (d, nγ)-reactions

A. Nilsson and I. Bergqvist
Institute of Physics, University of Lund, Lund

L. Nilsson
Atomic Energy Company, Studsvik, Nyköping

I. (d, nγ)- reactions in the atomic mass range 20 to 40

The primary purpose of this work was an investigation of the gamma transitions from bound isobaric analogue states of nuclei in the 2s1d shell by the use of (d, nγ) reactions.

Coincidences were registered between neutrons and gamma radiation produced in the (d, nγ) reaction. Neutrons were detected by an organic scintillator and the different neutron groups from the reaction were separated by time-of-flight techniques. The gamma radiation was detected by a NaI(Tl) scintillator 23 cm in diameter and 21 cm in length. The neutron detector was positioned in the forward direction to emphasize the excitation of $l_p = 0$ levels in the rest nucleus. This technique has been applied at a deuteron energy of 4 MeV in a study of the reactions $^{27}Al(d, n\gamma)^{28}Si$ and $^{31}P(d, n\gamma)^{32}S$. The decay of several T = 0 levels in ^{28}Si and ^{32}S have been observed as well as isobaric analogue states at 9.32, 9.38 and 11.42 MeV in ^{28}Si and 7.52 and 8.12 MeV in ^{32}S. The results obtained for ^{28}Si are in good agreement with recently published data from related (p, γ) observations. There do not exist any previous results on the 7.52 and 8.12 MeV transitions of ^{32}S. The (d, nγ) investigations agree very well with spin and parity values of 1^-, 0, 1^+ and 1^- of the 7.42, 7.52, 8.12 and 8.50 MeV levels, respectively, being in agreement also with observations of proton stripping reactions.

Because of the limited resolving power of the sodium iodide scintillator it is in many cases not possible to determine the position of a gamma transition with any certainty. The use of a Ge(Li) spectrometer would in many cases have been profitable. A 30 cm^3 Ge(Li) detector was recently used in a study of the $^{27}Al(d, n\gamma)^{28}Si$ reaction.

The flight path was chosen to be 1 m (compared to 3 m in previous experiments) to get a reasonable coincidence counting rate. The analyses of the data are in progress.

II. 2. Prompt gamma radiation from fission fragments

H. Albinsson
Chalmers Institute of Technology, Gothenburg

The prompt gamma radiation, emitted from fragments in slow neutron induced fission of ^{235}U, was studied as a function of fragment mass and time after fission. A gamma detector, a NaI scintillator, was placed about 70 cm from the fission foil in order to obtain time discrimination between the fission gammas and the prompt neutrons released in the fission process. The gamma radiation emitted in different time intervals after the fission events was studied by changing the position of a collimator along the path of the fission fragments.

The experiment was shut down in December 1969 because of reactor channel modifications. Shortly before the shut down a series of measurements was performed to study the yield of the prompt photons from the fragments as a function of mass and the total fragment kinetic energy. The main purpose of doing a study of this type is to try to gain some knowledge on the spin distribution in the fragments. Another way of looking at the problem is to say that the energy balance of the fissioning nucleus is studied. The release of the fission gamma radiation is, like the release of the prompt neutrons, a measure of part of the excitation energy available in the fragments. So far very few experiments have been tried with the same purposes.

In this measurement a lead collimator for the gamma radiation was used and so a real mass separation was performed. Early investigations have been done without a collimator and in reality the gamma radiation has been recorded in coincidence with the mass ratio, even though in a comprehensive analysis one is able to extract considerable information of the gamma yield as a function of fragment mass.

As a result of the present measurement it can be mentioned that the total gamma-ray energy decrease when the total fragment kinetic energy is changed from 160 to 200 MeV is about 2.7 MeV. In the few cases in the literature when values of this kind have been given, it has been the rate of gamma-ray energy decrease with increase in total fragment kinetic energy. The present experiment gives $-0.0084\ \mathrm{MeV}^{-1}$, within the uncertainty given from another experiment, in which no gamma collimation was used.

By changing the position of the collimator it was possible to get estimates of the life-times of the gamma-emitting states. One value earlier reported as tentative has now been established to be 50 ± 3 ps. This value has not been reported by any other group, even though it can be seen in earlier decay curves of ^{252}Cf.

Gamma-ray energy spectra as functions of mass have been accumulated with the collimator set to enhance the gamma radiation with the half-life of 50 ps. The yield of the gamma rays of different energies was varying in an interesting way. The yield of 1200 keV photons as a function of fragment mass showed pronounced structure with large yields in mass regions $A < 82$, ≈ 92 and ≈ 130. These mass regions corresponds to closed and almost closed nucleon shells, namely $N \approx 50$ for $A \approx 82$ and $Z \approx 50$ and $N \approx 82$ for $A \approx 132$. $A \approx 92$ is just below $Z \approx 40$. In the gamma-ray energy spectrum integrated over the whole mass spectrum, the 1200 keV distribution stands out very clearly. That these photons are important is clear from the fact that even in the uncollimated gamma-ray energy spectrum over all masses the 1200 keV photons are also seen as a bump. This is a remarkable thing as this spectrum contains a variety of photons.

One of the purposes of studying the gamma-ray energy spectra from the radiation, where the 50 ps component was enhanced, was to try to look for octupole radiation. It is reasonable to assume that some fragments should release this type of radiation, as some of them might be formed with pear shapes. The expected energy range in which these photons should be found is about 2-3 MeV. The spectra did not reveal any significant peaks or bumps in this energy range. This does not necessarily mean that these photons do not exist, but more experiments than this preliminary one are needed to clear up the situation.

II.3. The ^{137}I delayed neutron energy spectrum

S. Shalev and G. Rudstam
The Swedish Research Councils' Laboratory, Studsvik, Nyköping

Recent measurements [1] of group 2 (22 seconds) delayed neutron energy spectra have shown their essentially discrete nature. The line structure becomes more pronounced for heavier fissioning nuclei such as ^{238}U and ^{239}Pu, due to the relative displacement of the light mass peak in the mass-yield curve, and the increasing dominance of a single precursor - ^{137}I.

The OSIRIS on-line isotope separator [2] has been used to study the delayed neutron energies in the decay ^{137}I - ^{137}Xe - ^{136}Xe. The ion source, containing a ^{235}U layer on graphite, is located near the core of a 1 MW reactor. The mass-separated ions are collected on a tape and transported to the vicinity of a ^{3}He ionization spectrometer. During the measurement a new sample is collected on the tape, and for both collection and measurement times equal to 60 seconds this arrangement gives an average counting rate of 34 % of the saturation counting rate.

The neutron spectrometer had a detection efficiency of $1.1 \cdot 10^{-4}$ for 1 MeV neutrons emitted isotropically at the sample position. Energy resolution was in the range 16 keV to 28 keV FWHM for neutrons with energies up to 1 MeV. The spectrometer was shielded with cadmium and boral sheets, and mounted on a vibration-free stand. The electronic system comprised an Ortec 120-3 preamplifier and gaussian amplifier dc coupled to a biassed amplifier and a 4096 channel analyzer, with digital stabilization on both zero and gain. Routing 4 quarters of the analyzer at 0, 5, 20 and 40 seconds after sample arrival gave a crude measurement of the time dependence of the pulse-height spectrum.

The data were collected during a 10 hour measurement, with another 7 hours for background determination. This amounted to 39 %

---

[1] Shalev, S., Measurements on Delayed Neutrons from Fast Fission. Technion Israel report TNSD-R/412, Progress Report No. 4 (1970).

[2] Borg, S., Bergström, I., Holm, G.B., Rydberg, B., De Geer, L.-E., Rudstam, G., Grapengiesser, B., Lund, E. and Westgaard, L., On-line separation of isotopes at a reactor in Studsvik (OSIRIS). Nucl. Instrum. Methods 91 (1971) 109.

of the fast neutron counts, and the corrected spectrum is shown in Fig. 1. The effect of finite spectrometer resolution and detection efficiency (which is very high below 100 keV) have not been allowed for. The measured half-life of 26 ± 2 seconds is in agreement with the accepted [3] value of 24.4 ± 0.4 seconds.

The line structure and overall shape of the experimental spectrum are not in agreement with the energy distribution predicted by Gauvin and de Tourreil [4]. It would appear that the importance of spin and parity selection rules is much greater than had been assumed. In fact, a relatively simple neutron spectrum is expected in the case of ^{137}I. Assuming a $7/2^+$ ground state, allowed β-transitions lead only to d-wave neutron emission from $5/2^+$ levels in ^{137}Xe, and this is in strong competition [5] with γ-emission for energies below about 1 MeV.

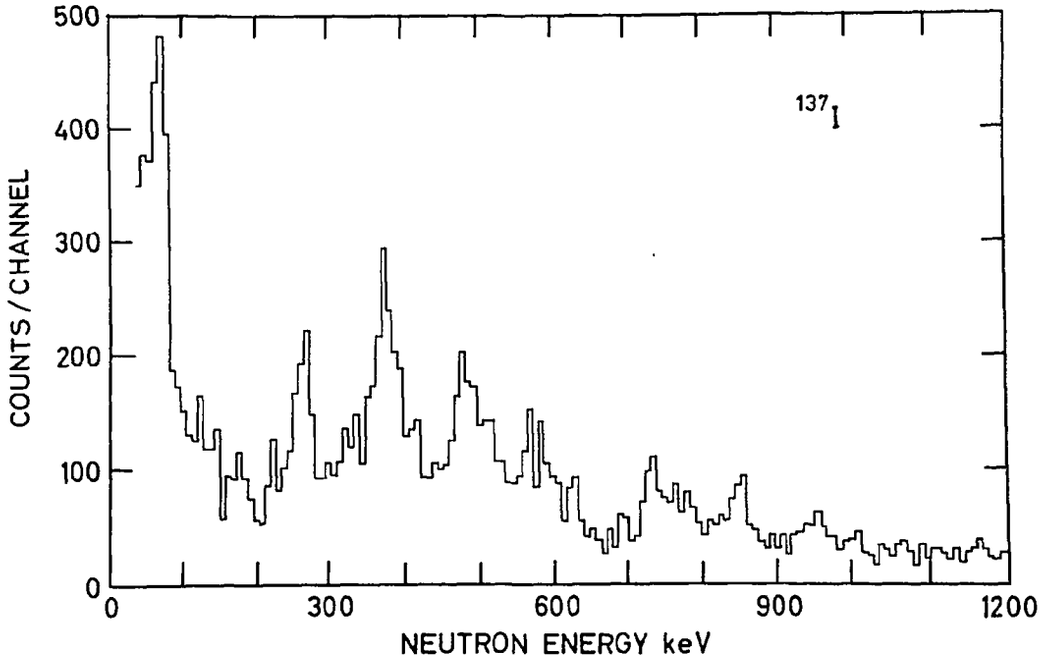

Fig. 1 Spectrum of delayed neutrons from I^{137}.

[3] Perlow, G. J. and Stehney, A. F., Halogen delayed-neutron activities, Phys. Rev. 113 (1959) 1269.

[4] Gauvin, H. and de Tourreil, R., Emission de neutrons retardes: Calcul des spectres d'énergie et des probabilités d'émission des précurseurs. Physics and Chemistry of Fission. Proc. of the 2nd IAEA Symposium. Vienna, 28 Jul. - 1 Aug. 1969. IAEA, Vienna 1969. p. 621. (STI/PUB/234).

[5] Jahnsen, T., Pappas, A. C. and Tunaal, T., Delayed neutron emission, theory and precursor systematics. Delayed Fission Neutrons. Proc. of a panel. Vienna, 24 - 27 Apr. 1967. IAEA, Vienna 1968. p. 35 . (STI/PUB/176).

II. 4. Studies of (d, pγ)-reactions

I. Bergqvist, L. Carlén and L. Nauclér
Department of Physics, University of Lund, Lund

B. Lundberg
Research Institute of National Defence, Stockholm

L. Nilsson
Tandem Accelerator Laboratory, Uppsala

With the aim to achieve an understanding of the neutron capture mechanism in nuclei with mass numbers around 60, (d, pγ)-reactions have been studied in ^{58,60}Ni and ^{63,65}Cu at 5.5 MeV deuteron energy. The gamma-rays were detected by a NaI(Tl) scintillator, 12.7 cm in diameter and 10.2 cm long, and the protons by a silicon surface-barrier detector of high resistivity. With the use of two-parameter multichannel analysis it was possible to record simultaneously the gamma-ray spectra from several excitation energy regions populated by neutron transfer, in particular those below the neutron binding energies. The gamma-ray spectra from excitation energy regions not too far below the neutron separation energy show strong-intensity high-energy gamma-rays. The shapes of the spectra are similar to those obtained in (n, γ)-reactions and disagree with those expected from the theory of the compound-nucleus capture process. A report on the experiment has been published previously.

The (d, pγ)-studies are being extended to chromium and iron isotopes and also to the A=90 mass region. Selfsupporting targets of natural iron (91.66 % ^{56}Fe), natural chromium (83.76 % ^{52}Cr) and yttrium (100 % ^{89}Y) have been delivered and enriched ^{54}Fe targets are being prepared. Preliminary experiments on natural iron and yttrium have been performed. In a recent two-parameter (d, pγ)-experiment at 5.0 MeV deuteron energy on natural iron, gamma-ray spectra were recorded by a large NaI(Tl) scintillator, 22.6 cm in diameter and 20.8 cm long. Preliminary analysis of the data shows that the shapes of gamma-ray spectra from excitation energy regions slightly below the neutron binding energy are similar to those obtained in neutron capture in the region 10 to 100 keV.

This experiment will be moved to the Tandem Accelerator Laboratory in Uppsala, where it will become possible to investigate a larger mass region. Furthermore, it is planned to use a Ge(Li) detector as a gamma-ray spectrometer.

II. 5. Lifetime measurements *

R. Hellborg
Atomic Energy Company, Studsvik, Nyköping

Measurements of the compound nuclei lifetime at neutron induced fission in uranium are going on. The angular distribution of fission fragments emitted from uranium dioxide single crystals bombarded with neutrons has been measured by using glassplates. If the lifetime of the nuclei is very short the fission fragment will be emitted when the compound nucleus is still at the lattice position. Then the fragment can not leave the crystal along axial or planar directions. On the other hand if the lifetime of the compound nucleus is very long it will leave the lattice position before the fission. The emitted fragments are not prohibited in any axial or planar direction and the detected distribution is isotropic. If the lifetime is of the order of the time it takes the nuclei to move the critical distance for channeling ($\sim 10^{-10}$ m) it is possible to calculate the lifetime from the detected fission fragment distribution.

The result of an experiment with 2.8 MeV neutrons gave an upper limit for the lifetime of $< 5.10^{-17}$ sec. i.e. with this neutron energy the compound nucleus lifetime is too short to be measured with this method. New experiments are planed using lower neutron energy i.e. lower excitation energy and longer lifetime of the compound nucleus.

---

* In collaboration with Det Fysiske Institut, Aarhus Universitet, Denmark.

III. THEORETICAL PHYSICS

III. 1. Level densities of spherical nuclei from exact counting of shell model states

J. Eriksson
Atomic Energy Company, Studsvik, Nyköping

S. Jägare
Research Institute for Physics, Stockholm

Simple exponential type Fermi gas parametrizations $\rho_{FG}(U)$ of the nuclear level densities at excitation energy U are most commonly applied in nuclear reaction cross section calculations. Intrinsically the derivation of $\rho_{FG}(U)$, or $\rho_{FG}(U,I)$ with the nucleus spin I included, utilized simplifying physical assumptions as well as some approximate mathematical methods. The evident shell structure of the nucleus is not considered in this type of parameterization and also the pairing energy is excluded from the formulation. These two effects, however, manifest themselves by varying values of the parameters of the $\rho_{FG}(U)$ and are thus, in a minor way, entering the level density of the individual nucleus. To effect the necessary improvements, i.e. to avoid as much as possible the usual physical and mathematical approximations, we calculate the energy dependent level densities $\rho(E)$ by the method of exact counting of the shell model states. By spin summation we further obtain the spin-distributed level density $\rho(E,I)$. It turns out that the model leads to level densites $\rho(E)$ which in mean are close to the $\rho_{FG}(U)$ obtained with good average parameters but that there is an apparent structure with energy.

Particular attention must be paid to the energies of the shell model levels. These energies are, in the particle picture, expressed by the standard pairing Hamiltonian. Identifying excitations as being quasiparticle excitations we should in each state really make a complete BCS-calculation, eventually with blocked levels. This would be too time-consuming since there are millions of states and each individual state must be solved by an iterative procedure. Instead we extend the simple free quasiparticle Hamiltonian by including some further terms from the transformation from the particle picture.

The terms which are

(a) not quasiparticle number conserving and

(b) non-diagonal in the quasiparticle-quasiparticle interaction

are excluded. Then we have the approximate Hamiltonian

$$H' = 2 \sum_{k>0} \epsilon_k V_k^2 + \sum_{k>0} \epsilon_k (U_k^2 - V_k^2)(\alpha_k^+ \alpha_k + \alpha_{-k}^+ \alpha_{-k}) +$$

$$+ G \sum_{\substack{k>0 \\ k>0}} \Big\{ U_k V_k U_{k'} V_{k'} \Big[-1 + (\alpha_k^+ \alpha_k + \alpha_{-k}^+ \alpha_{-k}) +$$

$$+ (\alpha_{k'}^+ \alpha_{k'} + \alpha_{k'}^+ + \alpha_{-k'}^+ \alpha_{-k'}) -$$

$$- (\alpha_k^+ \alpha_k + \alpha_{-k}^+ \alpha_{-k})(\alpha_{k'}^+ \alpha_{k'} + \alpha_{-k'}^+ \alpha_{-k'}) \Big] -$$

$$- U_k^2 U_{k'}^2 \alpha_k^+ \alpha_{-k}^+ \alpha_{-k'} \alpha_{k'} - V_k^2 V_{k'}^2 \alpha_{-k} \alpha_k \alpha_{k'}^+ \alpha_{-k'}^+ \Big\}$$

with common notations and the α^+ and α the quasiparticle creation and annihilation operators. From a number of test runs it was found that this Hamiltonian evidently is much better than the simpler free quasiparticle Hamiltonian.

Calculations of the level densites are in progress for several mass regions.

III. 2. Calculations of inelastic scattering cross sections

J. Eriksson

Atomic Energy Company, Studsvik, Nyköping

A reason for searching for refined level-density expressions is their importance in estimating inelastic neutron cross sections from the compound nucleus model. Attempts to make such calculations have recently been initiated. Preliminary results indicate that, in the energy region above some 5 MeV neutron energy, cross sections calculated in this way are of the correct order. At the low-energy end, however, there are indications that collective levels are

missed. Efforts are for this reason being made to include also the collective levels in the exact counting level model.

III. 3. A slow neutron scattering routine from the gas model

J. Eriksson
Atomic Energy Company, Studsvik, Nyköping

The assumption of zero-range isotropic neutron scattering in the center of mass system is extensively used in applying the Monte Carlo method on space flux calculations. With a scatterer Maxwellian energy distribution the differential cross section may be written

$$\sigma(p, q) = \alpha^2 \pi^{-1/2} p \exp(-q^2)$$

with α the scattering length parameter and (p, q) two parameters with simple relations to the laboratory system parameter pair (μ, Z) where μ is the scattering cosine and the Z gives the relative velocity change. The pair (p, q) are sampled in a region bound by straight lines.

III. 4. Generalized optical model parameters

J. Eriksson, B. Holmqvist and T. Wiedling
Atomic Energy Company, Studsvik, Nyköping

Reactor physicists frequently request total and elastic cross-sections which have not been measured or cross sections of elements which are rare or not naturally occurring such as fission products. To meet such requests the development of an interpolation procedure for optical model parameters is in progress. For this purpose a 12 parameter search procedure has been carried out with a parametization according to

$$\alpha = a_1 + a_2 A^{-1/3} + a_3 A^{-2/3} + I(a_4 + a_5 A^{-1/3} + a_6 I) +$$
$$E(a_7 + a_8 A^{-1/3} + a_9 I) + \delta\,(a_{10} + a_{11} A^{-1/3} + a_{12} I)$$

with α any optical model parameter (U, W, r_{oU}, r_{oW} or a) and with A the nucleon number, the neutron number N to proton number Z

assymetry coefficient $\bar{\imath} = (N-Z)/A$, the neutron energy E in MeV and with the δ being 0 for an even-even nucleus and increasing to 2 in the case of an odd-odd nucleus. Including 110 values of each optical model parameter, as obtained by Holmqvist et. al. [1] the following 12-component vectors $\vec{a}$ were found

$\alpha = U$: $\vec{a} = (40.827,\ 31.710,\ -15.118,\ 13.993,$
$208.40,\ -196.18,\ -0.2361,\ -0.1009,$
$0.2686,\ 0.2679,\ -4.6066,\ -10.919)$

$\alpha = W$: $\vec{a} = (16.798,\ -22.927,\ -16.055,\ 5.9877,$
$26.543,\ -202.68,\ -0.1685,\ 0.2291,$
$1.1197,\ 1.4872,\ -2.1718,\ -9.5042)$

$\alpha = r_{oU}$: $\vec{a} = (1.3741,\ -0.6253,\ -0.0972,\ -0.2540,$
$0.4773,\ 0.5341,\ 0.00289,\ 0.00172,$
$-0.0465,\ 0.0635,\ -0.1531,\ -0.0311)$

$\alpha = r_{oW}$: a = (1.2226, - 0.1486, 0.5720, - 0.4268,
0.00530, 4.7967, - 0.00192, - 0.00429,
- 0.0297, - 0.0187, 0.0902, - 0.0871)

$\alpha = a$: a = (0.5453, 0.3552, - 0.5528, 0.0365,
0.7347, 0.9040, 0.00786, 0.00503,
- 0.0372, 0.0506, - 0.1080, - 0.1971)

Also a search with only the 5 parameters a_1, a_2, a_3, a_6 and a_{10} nonzero was carried out.

These preliminary studies will be followed by more detailed ones.

---

[1] Holmqvist, B. and Wiedling, T., Neutron elastic scattering cross sections experimental data and optical model cross section calculations. 1969. (AE-366).

Holmqvist, B. et.al., A neutron elastic scattering study of chromium, iron and nickel in the energy region 1.77 to 2.76 MeV. 1970. (AE-385).

IV. VAN DE GRAAFF ACCELERATOR, STUDSVIK

IV.1. Accelerator performance

P. Tykesson
Atomic Energy Company, Studsvik, Nyköping

The Van de Graaff accelerator has been run with protons, deuterons and helium ions, with both DC beams and pulsed beams. The accelerator was run in two and three shifts for 5 days per week and the calculated total time available for experiments was 3200 hours, 3063 hours of which were used by scientists, 87 hours for machine tests and 50 hours were required for unforeseen maintenance.

The distribution of the available machine time between experiments performed by physicists from various institutes is shown in Table I and between different experimental branches in Table II.

Table I The distribution of the machine time for various institutes.

AB Atomenergi	58,7 %
Research Institute of National Defence (FOA)	17,3 %
Chalmers University of Technology	9,8 %
University of Lund	7,7 %
University of Aarhus, Denmark	4,2 %
University of Uppsala	2,3 %

Table II The distribution of the machine time for different experimental branches.

Neutron physics	52,7 %
Solid state physics	18,0 %
Nuclear physics	15,9 %
Materials physics	6,7 %
Irradiations	4,0 %
Machine tests	2,7 %

The unforeseen maintenance was mainly caused by sparks owing to serious tracks on the insides of the insulators in the accelerator tube. Because of the extensive inquiry for machine time, it was decided to short-circuit the bad insulators and continue to run the machine with the maximum voltage, i.e. 4,5 MV until the end of this year. The tube has been used since the installation of the accelerator in 1960 and has a running time exceeding 28.000 hours which must be considered as a very long time.

The number of normal breaks for maintenance of the machine have been four during the year, each generally consisting of one week.

A number of modifications have been carried out during the period, to improv the reliability and the operation of the machine. The most important modifications are as follows:

The vacuum rectifier tubes, type 6AF3, in the power supply for the ionization oscillator have been a source of error and have caused many shut downs of the machine in past years. Since it was not possible to get standard tubes with improved ratings which could be used inside the accelerator tank and the experience with silicon rectifiers in the top terminal was not encouraging, a new power supply was equipped with selenium rectifiers. Since the installation of the new power supply, one year ago, there have been no shut downs caused by failure of this unit.

To make it possible to change the ion source without letting air in to the accelerator tube a high vacuum valve has been installed in the drift tube in a position between the Focus 3 box and the entrance of the accelerator tube. This drift tube is a part of the klystron bunching system.

IV.2. "Dark current" measurements

P. Tykesson
Atomic Energy Company, Studsvik, Nyköping

The measurements were carried out with the purpose of giving an estimate of the "tails" around the bunched bursts. A simple arrangement with a post deflection system was used. By triggering

the system with the ion pulses from the machine and phasing the sinusoidal deflection voltage in time with the passing of the ion bursts between the deflection plates a time window as a function of the deflection voltage was obtained. The current in the beam outside the time window was measured on the deflection slits and by this way the "tails" around the bunched bursts could be determined.

The results show that as long as the width at half height of the pulse before bunching was < 20 ns, the "tails" around the bunched bursts was small i. e. about 6 % of the total beam current when the width of the pulse before bunching was 20 ns. However, if the width of the pulse before bunching was increased to 25 ns the "tails" increased to about 23 %. According to the theory for bunching with sine wave modulation wave forms about 28 % of the beam can be utilised in forming an ion burst within a time bracket of 1 % of the interval between bursts. This means it would be possible to bunch a pulse of a width of 28 ns. However, this presuppose an ideal rectungular wave form. Thus, in practice the limiting value of the width of the pulse before bunching is about 20 ns.

IV. 3. Crossed field analyser

P. Tykesson
Atomic Energy Company, Studsvik, Nyköping

A crossed field analyser having a magnetic field perpendicular to an electric field has been designed for use in the top terminal of the machine. With this arrangement it is possible to select the mass-to-charge-state ratio of the ion beam of the ion source before injecting the beam into the accelerator tube. The analyser will primarily be used to select the very small amount of doubly-charged helium ions delivered by the R. F. ion source. The physical dimensions of the analyser are such, that it can easily replace the klystron buncher normally installed.

The purpose of the terminal analyser is to make a rough selection of the desired beam before acceleration in order to decrease the tube loading. The final selection of the accelerated beam with high resolution is done with the accelerator analysing magnet.

Fig. 1 shows a mass-to-charge-state spectrum obtained beam in the bench test of the analyser when using ^{3}He in an R.F. ion source. Peaks of different ions are indicated as well as the positions of those not noticed owing to the low resolution of the analyser. Fig. 2 shows a spectrum of the beam through the accelerator analyzing magnet after proper adjustments of the crossed field analyser for maximum output of double-charged ^{3}He beam. The output of double-charged ^{3}He showed a large sensitivity to the gas pressure in the ion source and Fig. 3 illustrates a measurement in which the analysed $^{3}He^{++}$ beam has been observed as a function of the gas pressure measured in a position between the accelerator tube and the main vacuum pump. The double-charged helium beam was very well focused and could be transported without losses to a distant target position. The maximum analysed $^{3}He^{++}$ beam current was 0,5 μA. The ratio of the total beam through the tube to the analysed $^{3}He^{++}$ beam was then about 6. By allowing a higher value of this ratio and by using a gas feed system being cleaned of hydrogen it will be possible to increase the intensity of the double-charged ^{3}He beam.

When using the crossed field analyser with protons the resolution was good enough for complete separation of protons and molecular ions. I.e. when running the machine at 3MV and with a total beam of 78 μA at the entrance of the analysing magnet, the analysed proton beam was 76 μA.

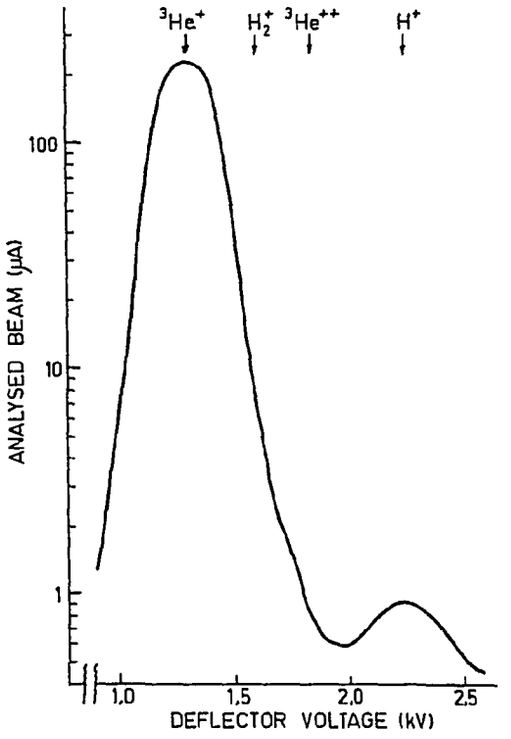

Fig. 1 A mass-to-charge-state spectrum obtained in the bench test of the analyser, when using ^3He in an R.F. ion source.

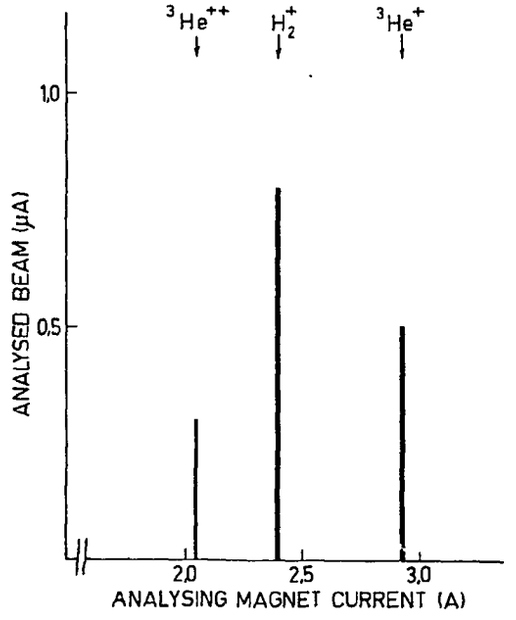

Fig. 2 A spectrum of the beam through the accelerator analysing magnet at the test of the crossed field analyser in the accelerator.

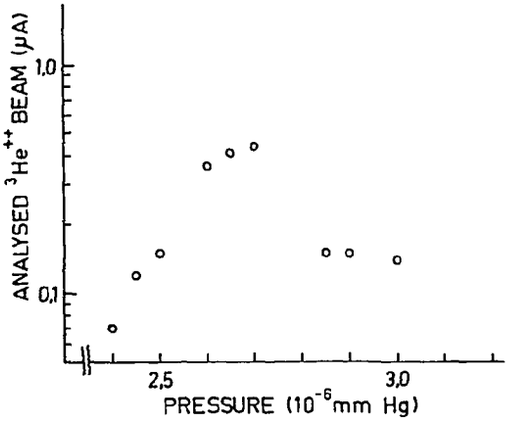

Fig. 3 The analysed $^3He^{++}$ beam as a function of the gas pressure.

V. REPORTS AND PUBLICATIONS

Atomic Energy Company, Studsvik, Nyköping, Sweden

Albinsson. H.
Prompt Gamma Radiation in Slow-Neutron Induced Fission of ^{235}U in Coincidence with the Total Fragment Kinetic Energy.
1970, AB Atomenergi, Sweden
(Internal report FN-10).

Albinsson, H. and Lindow, L.
Prompt Gamma Radiation from Fragments in the Thermal Fission of ^{235}U. 1970
(AE-398).

Albinsson, H.
Decay Curves and Half-Lives of Gamma-Emitting States from a Study of Prompt Fission Gamma Radiation. 1971
(AE-421).

Albinsson, H.
Energies and Yields of Prompt Gamma-Rays from Fragments in Slow-Neutron Induced Fission of ^{235}U. 1971
(AE-420).

Albinsson, H.
Studies of Prompt Gamma Radiation from Fission Fragments.
Dissertation, Gothenburg, 1971.

Almén, E., Holmqvist, B. and Wiedling, T.
Neutron Energy Spectra from Neutron Induced Fission of ^{238}U at 1.35 and 2.02 MeV,
Contribution to the IAEA Second International Conference on Nuclear Data for Reactors,
Conference Proceedings, Helsinki, 15 - 19 June, 1970.
Vol. II (1970) 93.

Almén, E., Etemad, M.A., Holmqvist, B. and Wiedling, T.
Fast Neutron Inelastic Scattering in the Energy Range 2 to 4.5 MeV,
Contribution to the IAEA Second International Conference on Nuclear Data for Reactors,
Conference Proceedings, Helsinki, 15 - 19 June, 1970.
Vol. II (1970) 349.

Almén, E., Holmqvist, B. and Wiedling, T.
Analyses of neutron scattering experiments,
In manuscript.

Almén, E., Holmqvist, B. and Wiedling, T.
Fission Neutron Spectra of ^{235}U and ^{238}U,
In manuscript.

Bergqvist, I., Lundberg, B. and Nilsson, L.
Cross Sections for High-Energy Gamma Transitions from MeV Neutron Capture in ^{206}Pb. 1970
(AE-388).
Nuclear Physics A153 (1970) 553.

Bergqvist, I. and Starfelt, N.
Neutron Capture γ-Rays,
Progress in Nuclear Physics Vol. 11 1 - 52,
Edited by D.M. Brinh and J.H. Mulvey, Pergamon Press, Oxford, 1970.

Eriksson, J.R.
Compound Nucleus Calculations of Low-energy Neutron Reaction Cross Sections Using Level Densities from Exact Counting of Shell Model States,
Contribution to the IAEA Second International Conference on Nuclear Data for Reactors,
Conference Proceedings, Helsinki, 15 - 19 June, 1970.
Vol. II (1970) 881.

Eriksson, J.R.
A Non-local Potential Approach in the Relativistic Nucleon-Nucleon Scattering,
Nuclear Physics A149 (1970) 501.

Eriksson, J.R.
A Slow Neutron Scattering Routine from the Gas Model,
Nuclear Science and Engineering 41 (1970) 307.

Hellborg, R.
The energy-loss of channeled protons determined in an indirect way,
To be published in Can. J. Phys.

Higbie, J.
Resolution of a solid state fission fragment mass spectrometer,
Nuclear Instruments and Methods 82 (1970) 253.

Holmqvist, B., Johansson, S.G., Lodin, G. and Wiedling, T.
Neutron Scattering from Vanadium at 1.5 to 8 MeV,
Nuclear Physics A146 (1970) 321 - 336.

Holmqvist, B., Johansson, S.G., Lodin, G., Salama, M. and Wiedling, T.
A Neutron Elastic Scattering Study of Chromium, Iron and Nickel in the Energy Region 1.77 to 2.76 MeV. 1970
(AE-385).

Holmqvist, B.
Experimental Nuclear Physics at the V.d.G. laboratory at Studsvik,
Contribution to the Nuclear Physics Conference at Lund, Lund, Sweden 1970.

Holmqvist, B. and Wiedling, T.
Fast Neutron Elastic Scattering at 8 MeV,
Contribution to the IAEA Second International Conference on Nuclear Data for Reactors,
Conference Proceedings, Helsinki, 15 - 19 June, 1970.
Vol. II (1970) 341.

Holmqvist, B. and Wiedling, T.
Neutron Elastic Scattering Cross Sections of Vanadium, Chromium, Iron and Nickel,
Contribution to the IAEA Second International Conference on Nuclear Data for Reactors,
Conference Proceedings, Helsinki, 15 - 19 June, 1970.
Vol. II (1970) 327.

Holmqvist, B., Wiedling, T., Benzi, V. and Zuffi, L.
Analyses of fast neutron elastic scattering from tantalum using a non-spherical optical potential,
Nuclear Physics A150 (1970) 105 - 113.

Holmqvist, B. and Wiedling, T.
Optical Model Descriptions of Fast Neutron Elastic Scattering Measurements,
In manuscript.

Holmqvist, B.
Some Viewpoints on Cross Section Standards and Related Problems for Fast Neutron Elastic and Inelastic Scattering Measurements.
Invited paper to EANDC Symposium on Neutron Standards and Flux Normalization at Argonne National Laboratory, U.S.A., on 21 - 23 October, 1970.
1970, AB Atomenergi, Sweden
(Internal report FN-13).

Holmqvist, B. and Wiedling T.
Optical Model Analyses of Neutron Scattering at 8 MeV,
Contribution to the American Physical Society,
Nuclear Physics Meeting, Houston, Texas, 15 - 17 October, 1970.
1970, AB Atomenergi, Sweden
(Internal report FN-14).

Lodin, G. and Nilsson, L.
The $^{16}O(d,n)^{17}F$ Reaction at Deuteron Energies from 2.5 to 5.5 MeV,
Zeitschrift für Physik 233 (1970) 181 - 194.

Nilsson, L. and Erlandsson, B.
A study of the $^{50}Cr(d,n)^{51}Mn$ and $^{54}Fe(d,n)^{55}Co$ reactions.
1969, AB Atomenergi, Sweden
(Internal report FN-4).

Nilsson, L., Nilsson, A. and Bergqvist, I.
The Decay of Bound Isobaric Analogue States in ^{28}Si and ^{32}S Using $(d,n\gamma)$ Reactions. 1970
(AE-386).
Physica Scripta 1 (1970) 161.

Nilsson, L.
Experimental Studies of Nucleon Capture and Transfer Reactions
Dissertation, Lund 1970.

Nilsson, L. and Erlandsson, B.
A Study of the $^{50}Cr(d,n)^{51}Mn$ and $^{54}Fe(d,n)^{55}Co$ Reactions,
Z. Physik 232 (1970) 303 - 324.

Tykesson, P. and Wiedling, T.
A Klystron Bunching System for a 6 MV Van de Graaff Accelerator,
Nuclear Instruments and Methods 77 (1970) 277 - 282.

Wiedling, T.
Fission Neutron Spectra, Microscopic Results.
Invited paper to EANDC Symposium on Neutron Standards and Flux Normalization at Argonne National Laboratory, U.S.A., on 21 - 23 October, 1970.
1970, AB Atomenergi, Sweden
(Internal report FN-12).

Research Institute of National Defence, Stockholm, Sweden

Bergqvist, I. and Lundberg, B.
Gamma-Rays from Neutron Capture in Mg, Si, P and S,
Physica Scripta 2 No. 6 (1970) 265 - 271.

Condé, H. and Holmberg, M.
Prompt $\bar{\nu}$ in Spontaneous and Neutron Induced Fission of ^{236}U and the Half-Life for Spontaneous Fission,
To be published in Journ. of Nucl. Energy.

Condé, H., Hansén, J. and Widén, L.
Proc. Symp. on Neutron Standards and Flux Normalization,
Argonne Oct. 1970, Conf-701002, paper 44.

Lundberg, B., Strömberg, L.G. and Condé, H.
Gamma-Rays from Inelastic Neutron Scattering in Oxygen,
To be published in Physica Scripta.

Nyström, G., Lundberg, B. and Bergqvist, I.
Neutron Capture Cross Sections in F, Mg, Al, Si, P and S from 20 to 80 keV,
FOA report C4440-22 Sept. 1970.

The Swedish Research Councils' Laboratory, Studsvik, Nyköping, Sweden

Borg, S., Bergström, I., Holm, G.B., Rydberg, B., De Geer, L.-E., Rudstam, G., Grapengiesser, B., Lund, E. and Westgaard, L.
On-Line Separation of Isotopes at a Reactor in Studsvik (OSIRIS),
Nucl. Instrum. Methods 91 (1971) 109.

Fogelberg, B. and Bäcklin, A.
Levels in ^{178}Hf Studied in the (n,γ)-Reaction,
Submitted to Nuclear Physics.

Shalev, S.
Measurements on Delayed Neutrons from Fast Fission,
Technion Israel report TNSD-R/412, Progress Report No. 4 (1970).